

Linear Accelerators: Theory and Practical Applications: WEEK 1



Stanford Linear Accelerator, shown in an aerial digital image. The two roads seen near the accelerator are California Interstate 280 (to the East) and Sand Hill Road (along the Northwest). Image data acquired 2004-02-27 by the United States Geological Survey



Roger M. Jones

**The University of Manchester, UK/
Cockcroft Institute, Daresbury, UK.**

March 12th – April 22nd, 2007.



Overview

This course introduces the fundamentals of linear accelerators ranging from Alvarez DTLs through to electron linear accelerators in the ILC. Both superconducting and room temperature linacs are presented in the lectures. Throughout the course, fundamental concepts such as conservation of energy are used. In particular, the following topics are discussed:

- . Phase stability
- . Beam focussing
- . Principal RF design parameters
- . Waveguide to cavity coupling
- . Globalised scattering matrix analysis
- . Tuning and modal stability
- . Steady state and transient beam loading.
- . Beam compensation schemes
- . Shunt impedance and 'R/Q' optimisation
- . Travelling wave accelerators (constant impedance and constant gradient)
- . Standing wave accelerators
- . RF pulse compression and SLED
- . Circuit analysis
- . Long-range and short-range wake-fields
- . Instabilities and beam dynamics
- . Emittance and phase space concepts
- . Current e.m. field computer codes and their range of applicability

Admin

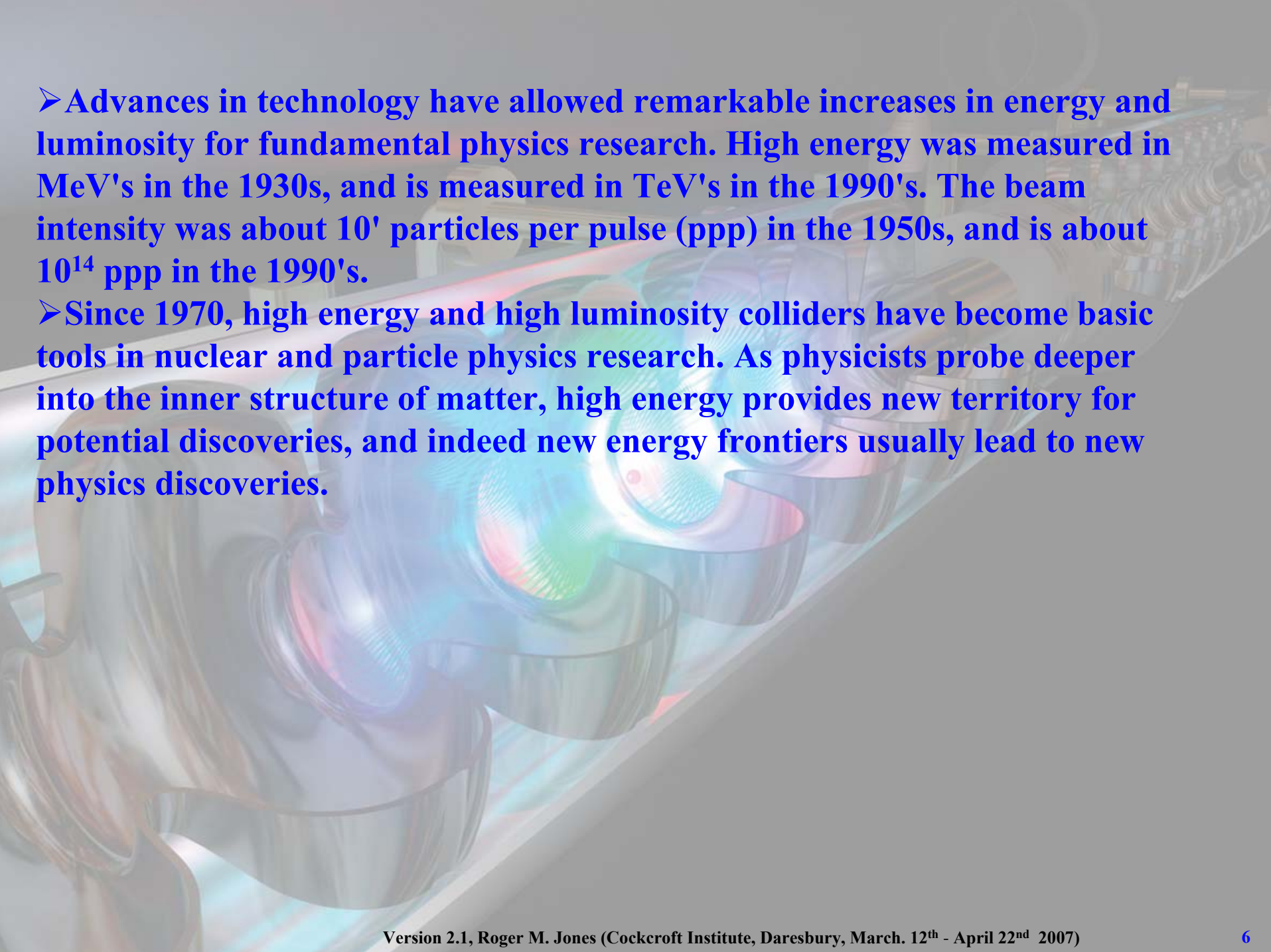
- The course in Weeks 2 and 3 will be supplemented with a tutorial using Superfish by Dr. Ian Shinton.
- All students are expected to perform the Superfish simulations for homework. The means to download the code and simulations tasks will be assigned in Week 2.
- In Week 3 the results of the simulations will be discussed. The accuracy of a circuit model in predicting the eigenmodes will be studied and compared with Superfish simulations.
- There will be no formal examination.
- General feedback on the overall course to:
r.m.jones@dl.ac.uk or Roger.Jones@Manchester.ac.uk.

References

- ❑ “Linear Accelerators”, North Holland Publishing Co. –John Wiley Interscience Div. (1970) eds. Pierre Lapostolle and Albert Septier.
- ❑ “The Stanford Two-Mile Accelerator”, W.A. Benjamin (1968) ed. Richard Neal.
- ❑ “RF Superconductivity for Accelerators”, Wiley Publishers (1998), by Hasan Padamsee, Jens Knobloch and Tom Hays.
- ❑ “Principles of Particle Accelerators”, W.A. Benjamin (1968) by Enrico Persico et al.
- ❑ “Particle Accelerators” McGraw Hill Book Co. (1962) by Stanley Livingston and John Blewett
- ❑ Principles of Charged Particle Acceleration John Wiley (1986) by Stanley Humphries
- ❑ “RF Linear Accelerators”, Wiley & Sons Publishers (1998), by Thomas Wangler.
- ❑ “Physics of Collective Beam Instabilities in High Energy Accelerators” , Wiley & Sons Publishers (1993) by Alexander Chao.
- ❑ “The Physics of Particle Accelerators: An Introduction”, Oxford University Press (2000) by Klaus Wille.
- ❑ “Fundamentals of Beam Physics” Oxford University Press (2003) by James Rosenzweig
- ❑ “Particle Accelerator Physics I & II”, (study edition) Springer-Verlag (2003) by Helmut Wiedemann.
- ❑ “Impedances and Wakes in High Energy Particle Accelerators”, World Scientific Publishers (1998), by Bruno W Zotter and Semyon Kheifets.

Introduction

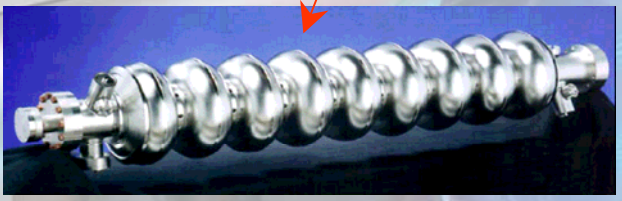
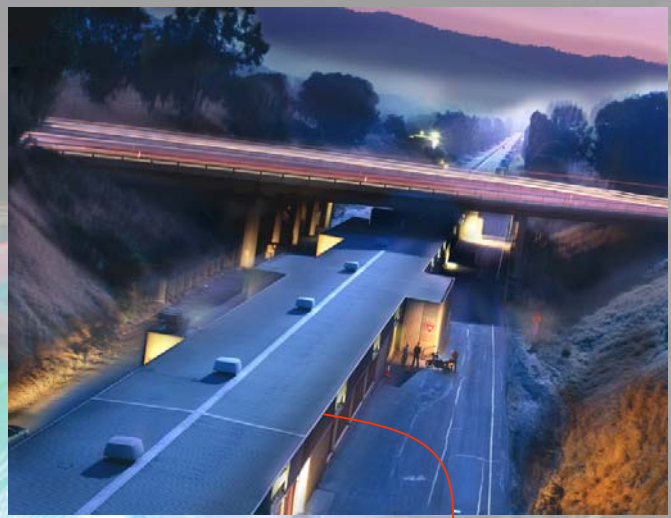
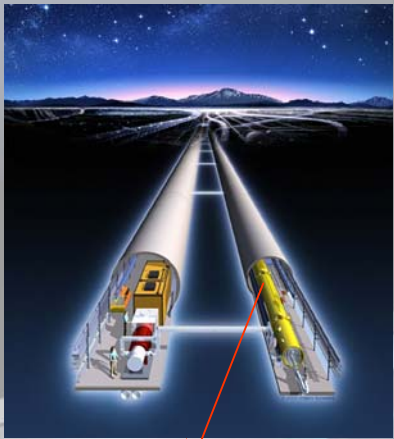
- The first accelerator dates back to prehistoric-historic times, when men built bows and arrows for hunting.
- The race to build modern particle accelerators began in 1911 when Rutherford discovered the nucleus by scattering α -particles off Aluminum foil. The physics and technology of accelerators and storage rings involves many branches of science. These include electromagnetism, solid-state properties of materials, atomic physics, superconductivity, nonlinear mechanics, spin dynamics, plasma physics, and quantum physics.
- In recent years, accelerators have found many applications: they are used in nuclear and particle physics research, in industrial applications such as ion implantation and lithography, in biological and medical research with synchrotron light sources, in material science and medical research with spallation neutron sources; etc.
- Accelerators have also been used for radiotherapy, food sterilization, waste treatment, etc. A major application of particle accelerators is experimental nuclear and particle physics research.



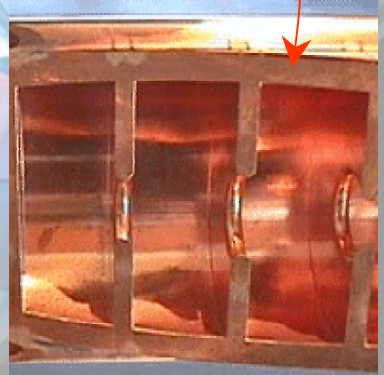
➤ **Advances in technology have allowed remarkable increases in energy and luminosity for fundamental physics research. High energy was measured in MeV's in the 1930s, and is measured in TeV's in the 1990's. The beam intensity was about 10^7 particles per pulse (ppp) in the 1950s, and is about 10^{14} ppp in the 1990's.**

➤ **Since 1970, high energy and high luminosity colliders have become basic tools in nuclear and particle physics research. As physicists probe deeper into the inner structure of matter, high energy provides new territory for potential discoveries, and indeed new energy frontiers usually lead to new physics discoveries.**

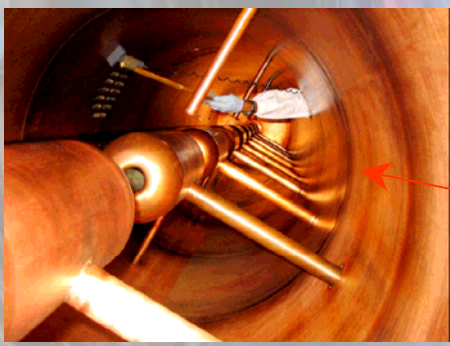
RF Linear Accelerators



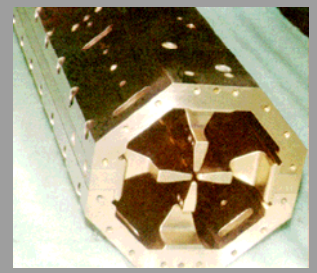
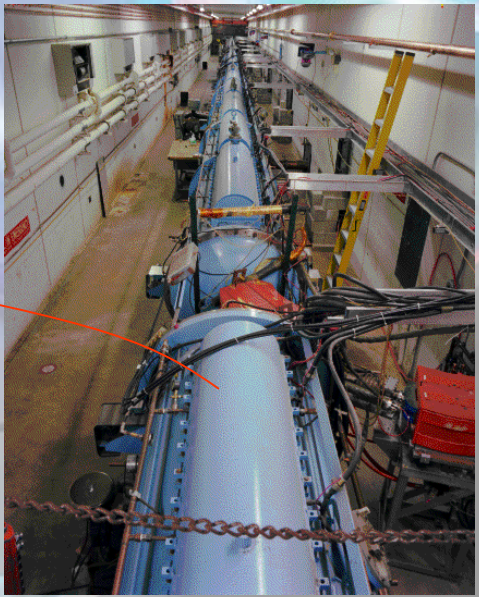
**ILC 9-cell Nb Cavity
Operating at 1.3 GHz.**



**SLAC 2.856 GHz
Cu Accelerator Cells**



**DTL tank #2 in the
Fermilab Linac operating
at 425 MHz**



**RFQ Operating
at 425 MHz**

Chronological Development

Cathode Ray Tubes
Late 1800s

Multipole Gaps
Cockcroft Walton (1920)

Van Der Graff (1930)

Electrostatic Field Based

Time Varying Field Based

Time Varying Fields
Ising (1924) and Wideroe

Cyclotron
Lawrence (1930)

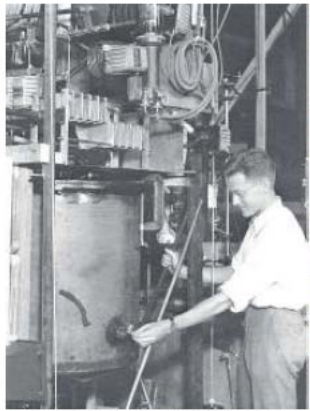
Synchrotron
Oliphant (1943)

Synchrocyclotron and Betatron
McMillan and Veksler (1944)

Alvarez Linac
McMillan (1946)

Strong Focusing
Courant and Snyder (1952)

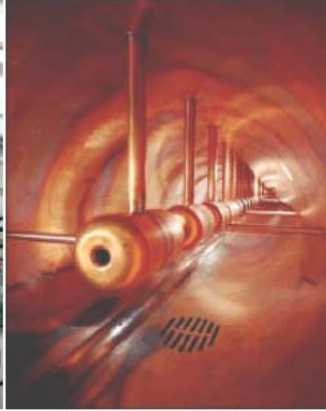
RF Linear Accelerators



D. Sloan and his 1 MeV LINAC



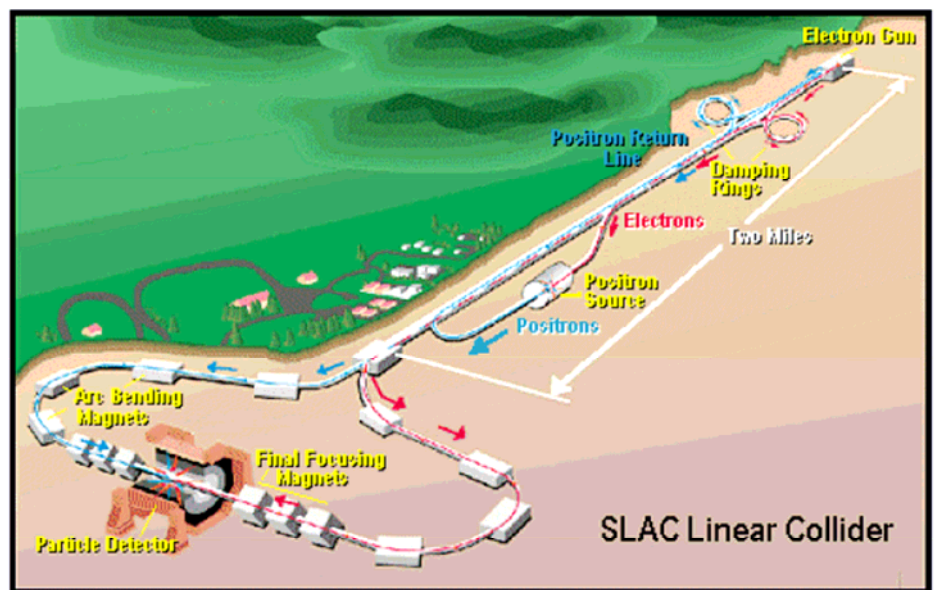
400 MeV LINAC at Fermilab (H ions)



Drift cells of Fermilab LINAC

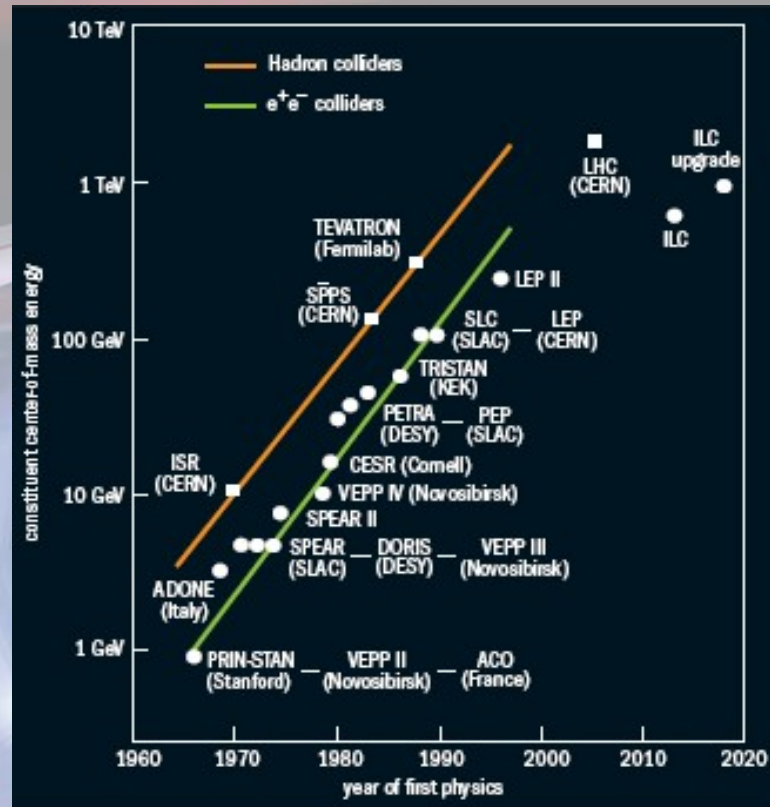
1931 D. Sloan (UC-Berkley, E.O. Lawrence group) builds a LINAC that could accelerate Hg ions up to 1 MeV. However, further research in this direction was set aside. It did not sound economical to escalate the number of accelerating gaps in comparison to the new idea of cyclotrons also being developed at Berkeley when particles were brought back to the same accelerating gaps by turning them around in magnetic field.

The idea will be revived again later when cyclotrons will hit their limitations. - Linear accelerators nowadays are a standard element of all modern accelerators (it follows the RFQ stage). - Also, there are some linear accelerators where the LINAC is the main thing: 45 GeV electron-positron LINAC at Stanford and 800 MeV proton LINAC at Los Alamos National Lab. These two are the largest in the world for the electrons and proton beams, respectively.



45 GeV electron-positron LINAC complex at Stanford

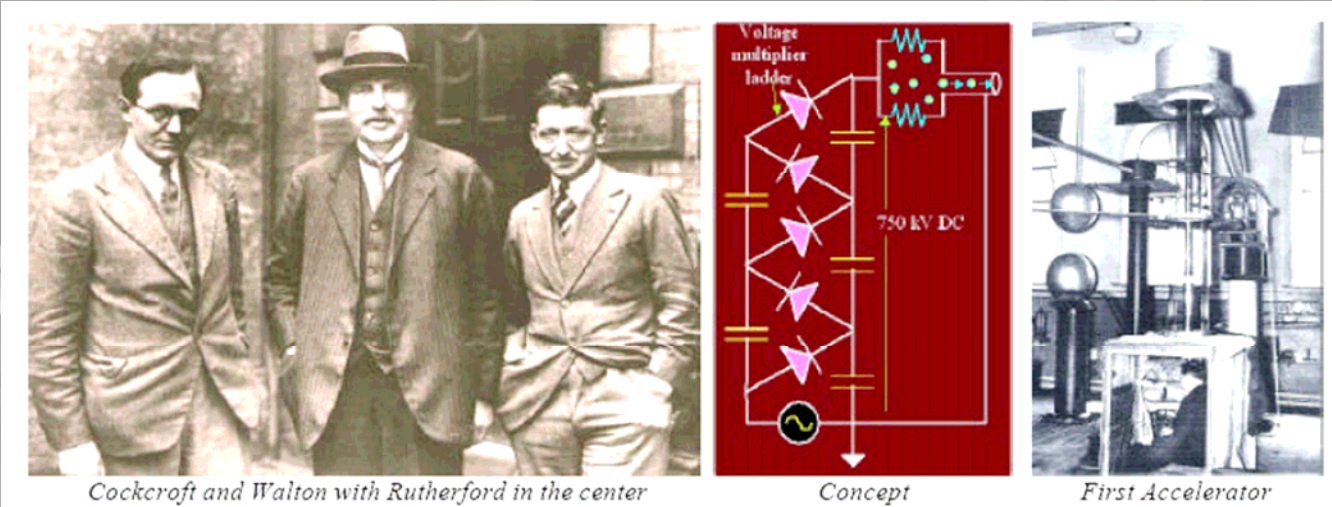
Livingston Curve



Computer scientists see the imminent end of Moore's law around 2020, the exponential growth in accelerator technology, described by the so-called Livingston curve, is perhaps also reaching its technical limit?

An adaptation of the "Livingston Curve," displaying the center of mass energies of the particle (parton) constituents of existing and planned accelerators (electron-positron and hadron colliders) as a function of the timeline. In the case of the hadron machines, energies have been adjusted to account for quark and gluon constituents. The original NLC (New Linear Collider) point has been updated to the ILC and its expected upgrade.

Potential-Drop Accelerators

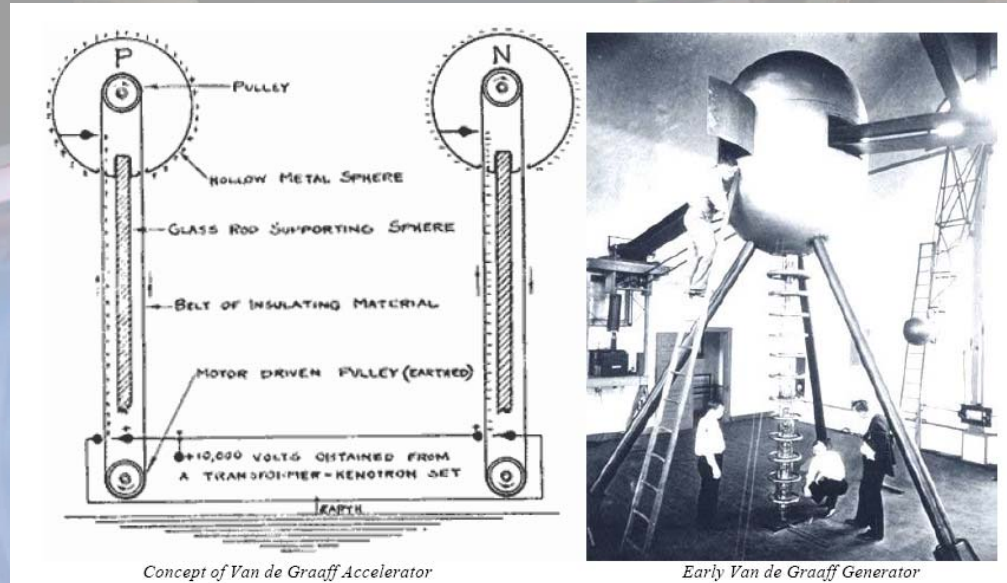


- **Accelerators: Cockcroft-Walton 1928-1932 D. Cockcroft and T. Walton (Rutherford's Lab in Cambridge) invented/applied a combination of large transformer combined with a rectifier to accelerate protons to a few 100 keV.**
- **1932 Cockcroft-Walton accelerator of 0.75 MeV: $p+Li \rightarrow He$ (first artificial element transmutation) Cockcroft-Walton accelerator is the first elements in most contemporary accelerators: Max Kinetic Energy ~ a few MeV**
- **1951 D. Cockcroft and T. Walton received Nobel Prize "for their pioneer work on the transmutation of atomic nuclei by artificially accelerated atomic particles"**

Potential-Drop Accelerators



Robert J. Van de Graaff



Concept of Van de Graaff Accelerator

Early Van de Graaff Generator

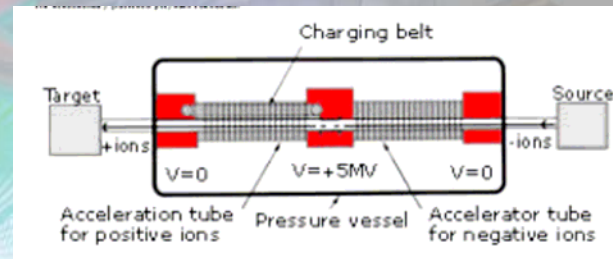
- 1929 Robert J. Van de Graaff (postdoc at Princeton) invents a high voltage generator and builds the first 80 kV model
- 1931 Two-sphere generator of -0.75 MV and +0.75 MV, to give total 1.5 MV
- 1933 Generator of 7 MV (MIT)

Potential-Drop Accelerators

Potential Drop Accelerators Employ Electrostatic Fields

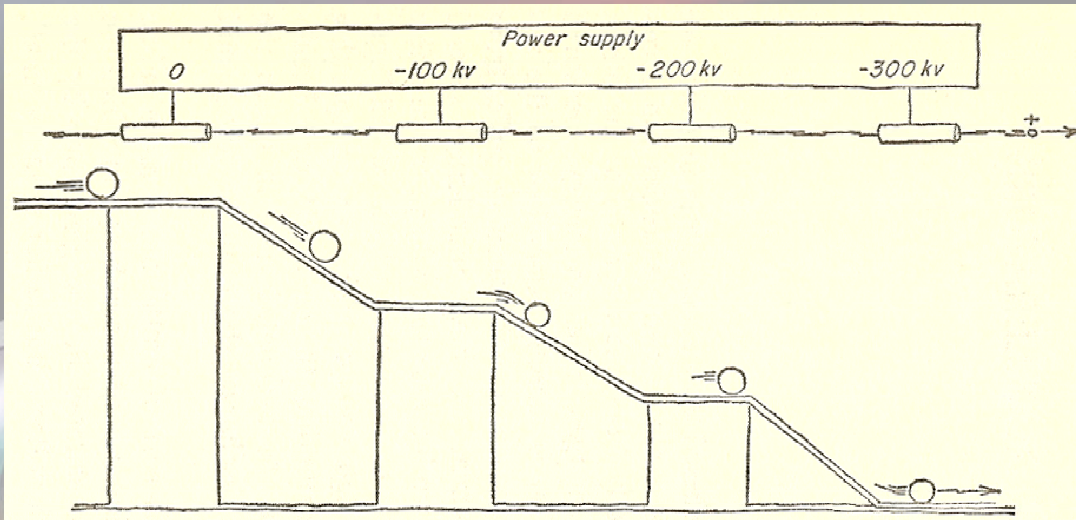
- The first high-voltage particle accelerator had a potential drop of the order of 100 kV and was conceived by and named Cockcroft Walton Accelerator in 1920.
- The most common potential-drop accelerator in use today is named after its inventor, the American Robert Jemison Van de Graaff. Nowadays most Van de Graaff accelerators are commercial devices and they are available with terminal voltages ranging between one and 25 million volts (MV)

In comparison the potential in clouds just before they are discharged by lightning is about 200 MV.



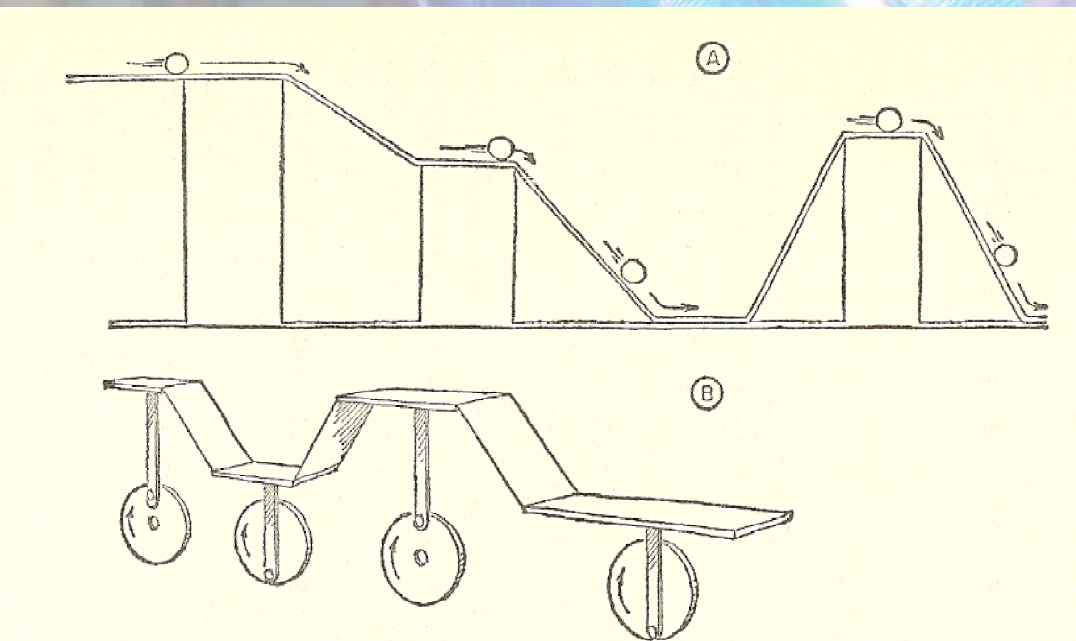
- One of the largest tandem accelerators was used for many years at Daresbury. Its acceleration tube, placed vertically, is 42 meters long and the centre terminal could hold a potential of up to 20 MV.

Mechanical Analogue to RF Linac



Bowling alley model of particle accelerator: gravity accelerates ball's motion on the sloping part of the track. The height of each horizontal section corresponds to a voltage source in the particle accelerator. The amount of acceleration is limited by the difference in levels between the top and foot of the entire track.

In the fixed track arrangement, A although it has some steep descents, the ball is required to climb the intermediate rises. Overall, the gain in speed is just the same as if the track had been laid out smoothly (as above). In B however, the horizontal sections move up and down, carrying the ball with them. With a judicious choice of timing, the ball can always be moving downhill between sections, never having to climb hills at all.

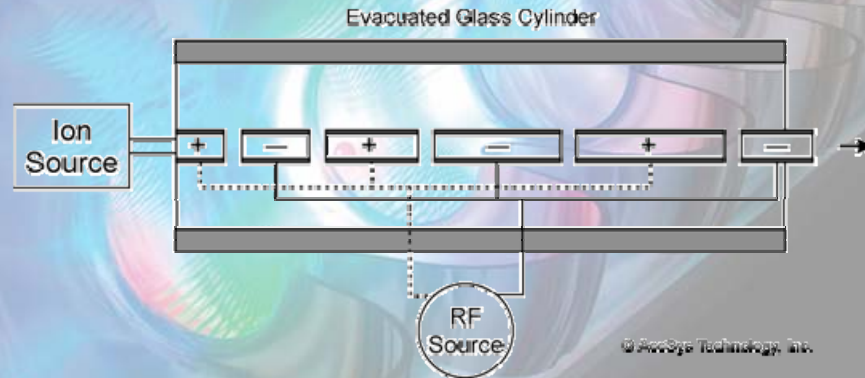


Birth of Linacs

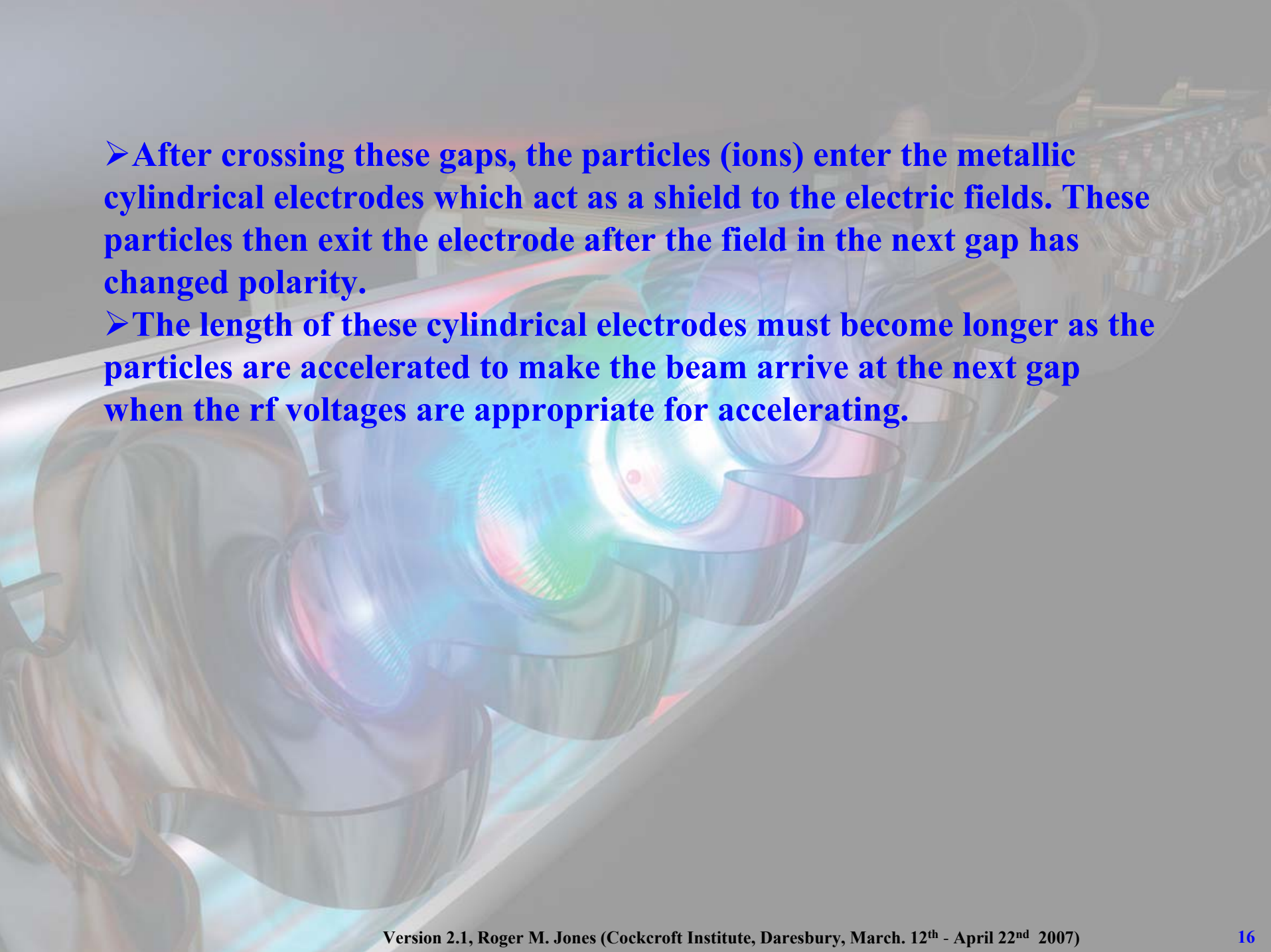
- The Cockcroft-Walton and Van de Graaff accelerators are machines with static field. Therefore, the acceleration of particles happens in one step.
- The linear accelerator employs the idea of kicking charged particle a few times (multi-stage acceleration), which requires quick alternation of potentials. Beam of particles necessarily becomes bunched. In 1929 Wideroe invents a multi-gap drift lineal accelerator (LINAC) and builds a small 3-stage prototype.

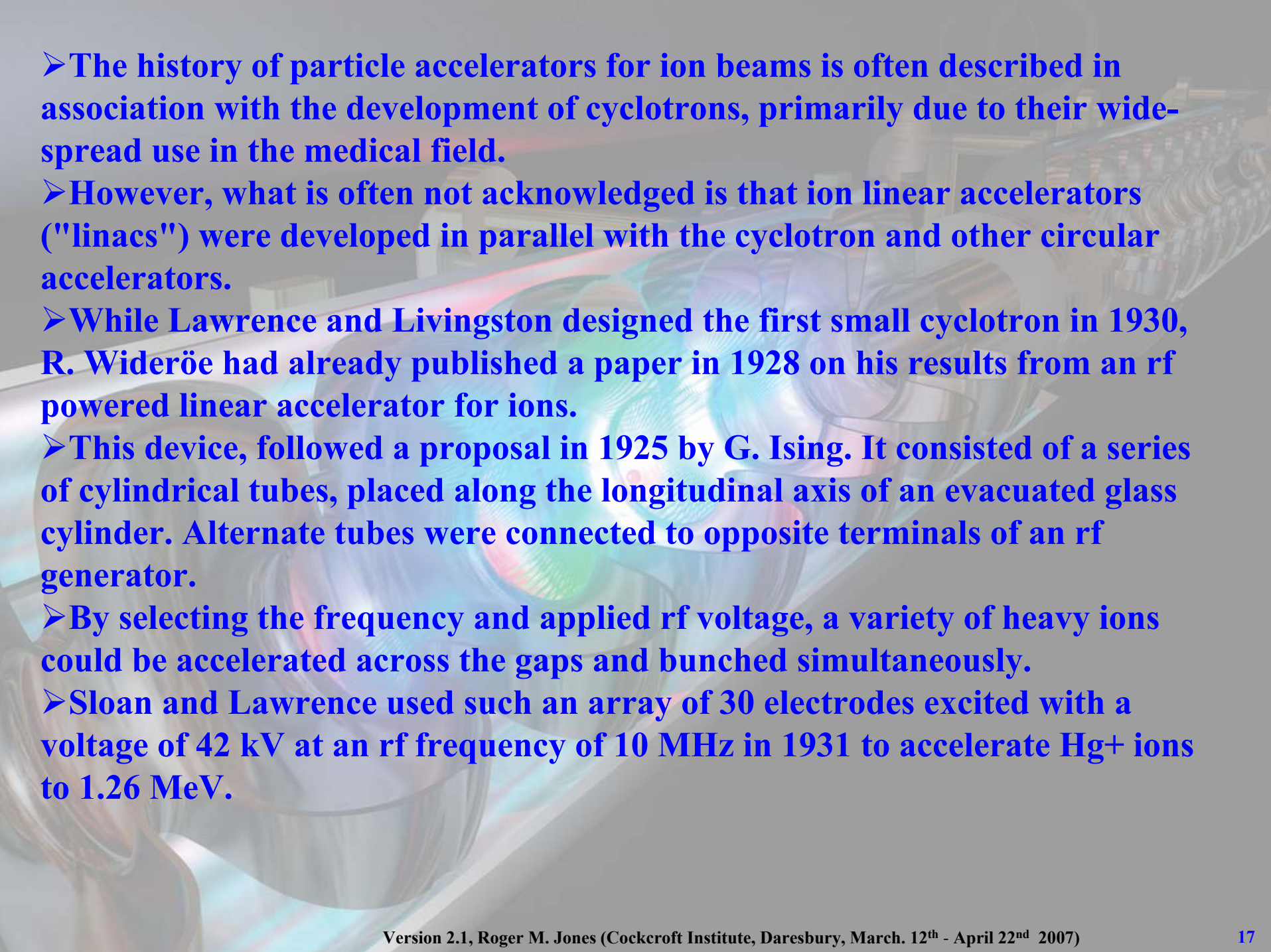


1929 Wideroe



- The ion velocity fits the criterion that the distance between the midpoint of each gap is given by $\frac{1}{2} v / c \cdot c / f \equiv \frac{1}{2} \beta \lambda$.
- The Wideroe design is a standing wave cavity in which the accelerating electric field maxima and nodes remain fixed in space. At a moment when the rf voltages are maximum on each electrode, acceleration takes place in every other gap.

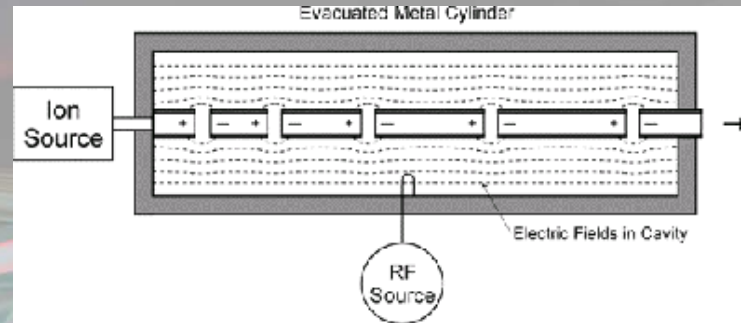
- 
- After crossing these gaps, the particles (ions) enter the metallic cylindrical electrodes which act as a shield to the electric fields. These particles then exit the electrode after the field in the next gap has changed polarity.
 - The length of these cylindrical electrodes must become longer as the particles are accelerated to make the beam arrive at the next gap when the rf voltages are appropriate for accelerating.

- 
- The history of particle accelerators for ion beams is often described in association with the development of cyclotrons, primarily due to their widespread use in the medical field.
 - However, what is often not acknowledged is that ion linear accelerators ("linacs") were developed in parallel with the cyclotron and other circular accelerators.
 - While Lawrence and Livingston designed the first small cyclotron in 1930, R. Wideröe had already published a paper in 1928 on his results from an rf powered linear accelerator for ions.
 - This device, followed a proposal in 1925 by G. Ising. It consisted of a series of cylindrical tubes, placed along the longitudinal axis of an evacuated glass cylinder. Alternate tubes were connected to opposite terminals of an rf generator.
 - By selecting the frequency and applied rf voltage, a variety of heavy ions could be accelerated across the gaps and bunched simultaneously.
 - Sloan and Lawrence used such an array of 30 electrodes excited with a voltage of 42 kV at an rf frequency of 10 MHz in 1931 to accelerate Hg⁺ ions to 1.26 MeV.

Drift Tube Linacs (DTL)



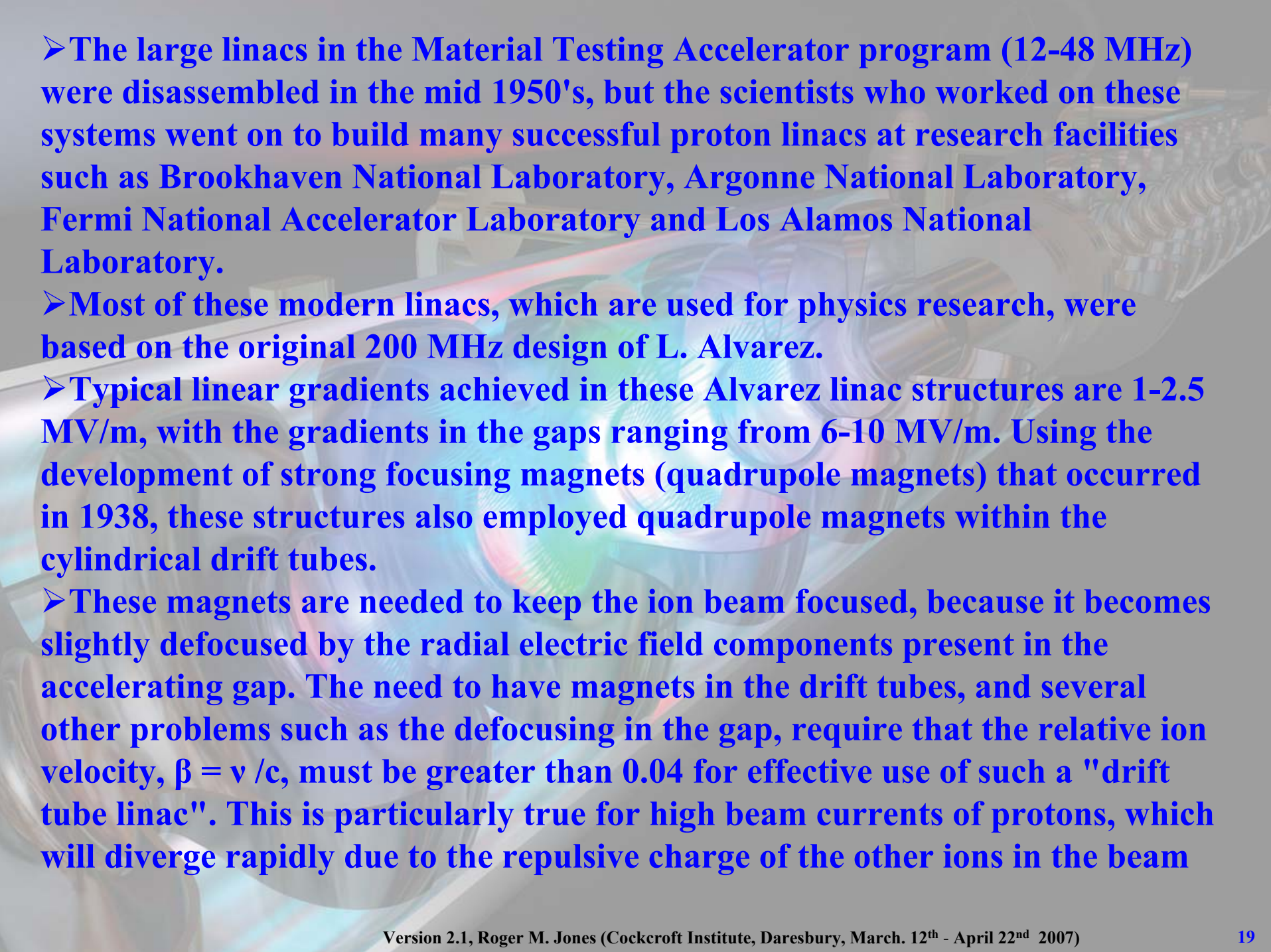
**Luis Alvarez ,
Inventor of the DTL.**



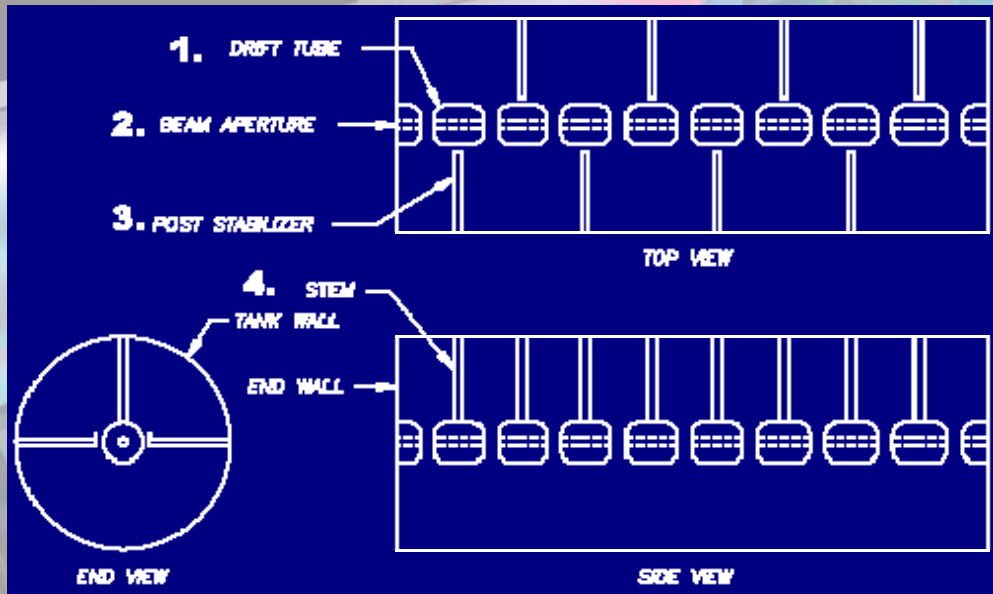
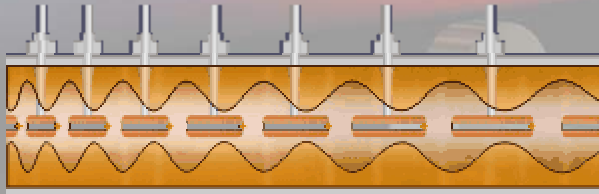
➤ In the late 1940's, after the second World War, a program was initiated by E.O. Lawrence at the University of California Radiation Laboratory (now known as the Lawrence Berkeley National Laboratory) with the US Atomic Energy Commission to investigate electronuclear breeding of Pu239, U232 and tritium by bombarding depleted uranium with accelerator-produced neutrons.

➤ A series of high power rf linacs for protons and deuterons was built and tested starting in 1950 at the site which is now the Lawrence Livermore National Laboratory.

➤ When the first linac was built, the only other proton linac which had been operated was the 32 MeV linac built by L. Alvarez, although a 68 MeV p+ linac was under construction at the University of Minnesota.

- 
- The large linacs in the Material Testing Accelerator program (12-48 MHz) were disassembled in the mid 1950's, but the scientists who worked on these systems went on to build many successful proton linacs at research facilities such as Brookhaven National Laboratory, Argonne National Laboratory, Fermi National Accelerator Laboratory and Los Alamos National Laboratory.
 - Most of these modern linacs, which are used for physics research, were based on the original 200 MHz design of L. Alvarez.
 - Typical linear gradients achieved in these Alvarez linac structures are 1-2.5 MV/m, with the gradients in the gaps ranging from 6-10 MV/m. Using the development of strong focusing magnets (quadrupole magnets) that occurred in 1938, these structures also employed quadrupole magnets within the cylindrical drift tubes.
 - These magnets are needed to keep the ion beam focused, because it becomes slightly defocused by the radial electric field components present in the accelerating gap. The need to have magnets in the drift tubes, and several other problems such as the defocusing in the gap, require that the relative ion velocity, $\beta = v/c$, must be greater than 0.04 for effective use of such a "drift tube linac". This is particularly true for high beam currents of protons, which will diverge rapidly due to the repulsive charge of the other ions in the beam

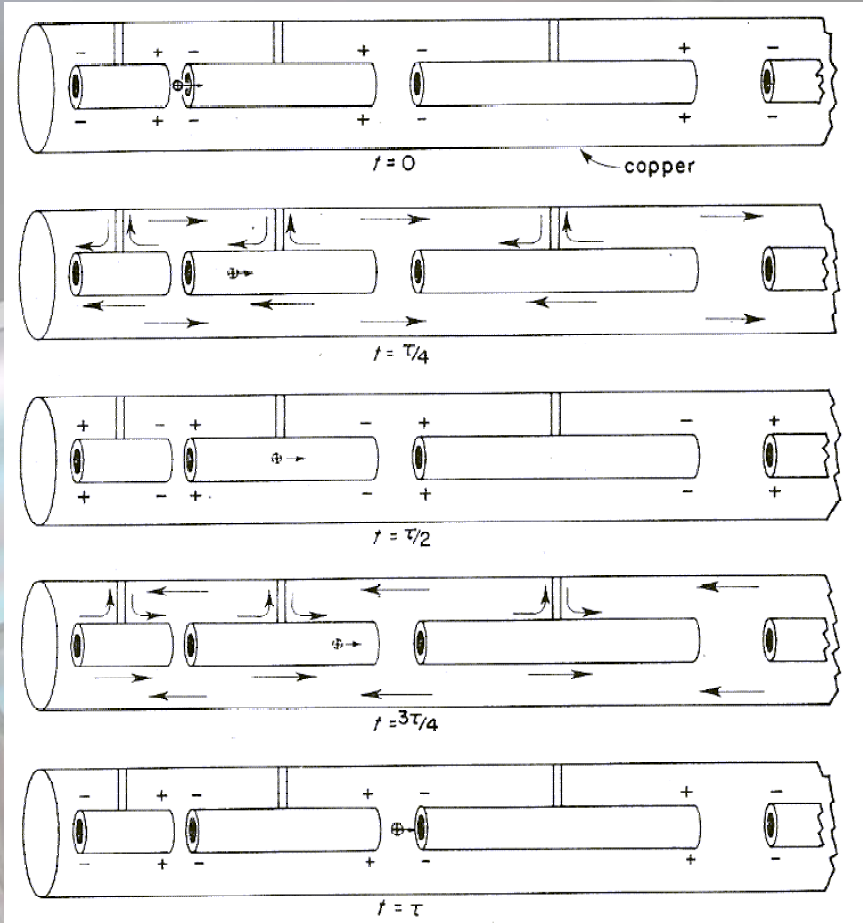
Drift Tube Linacs (DTL)



Fundamental Principles of DTL Operation:

1. A radio frequency system, such as a klystron or IOT, produces high electric fields in the gaps between electrodes.
2. The electric fields in each gap oscillate together at the frequency of the rf power.
3. The charged particles arrive in bunches, timed to enter the first gap when the field is accelerating.
4. When the field is reversed, *i.e.* decelerating, the particles are hidden in the bore of the drift tube, shielded from the electric field.
5. The drift tube length and spacing increases to keep pace with the increasing particle velocity as they gain energy.
6. The bunches are timed to arrive in the center of the gap, as the field is increasing, so that those arriving early gain less energy, and those arriving late gain more energy.
7. The beam is focused in the transverse direction by strong permanent magnet quadrupoles inside each drift tube.

Drift Tube Linacs (DTL)



Alvarez DTL. Ions travel from gap to gap in a full period of the rf field. Arrows indicate the charging currents.

- The electric field polarises the drift tubes so that periodically the two ends are charged to opposite sign.
- When charging currents flow to the right along the tubes, an equal current flows to the left along the inside wall of the outer cylinder.
- The tubes are supported at their centers by radial rods along which no current flows.

Drift Tube Linacs (DTL)

➤ This is known as a DTL ‘beta-lambda’ linac – the length of the nth cell is given by: $L_n = \beta_n \lambda$.

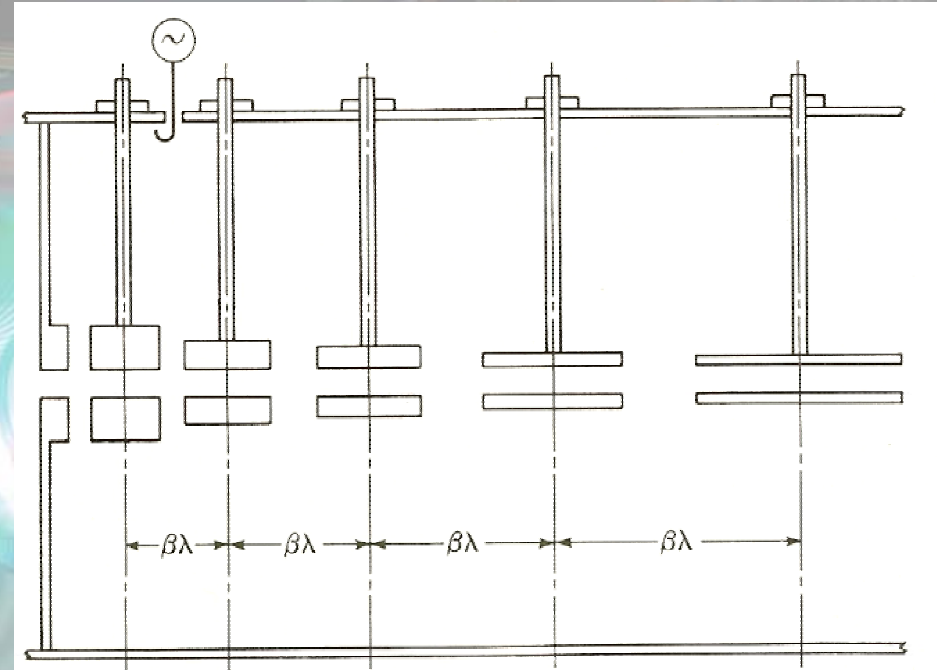
The energy at any cell in this Alvarez linac is obtained from the ‘beta-lambda’ length

$$\text{of each cell : } L_n^2 / \lambda^2 = \beta_n^2 = (E_n^2 - E_0^2) / E_n^2 \\ = 1 - E_0^2 / (T_n + E_0)^2$$

$$\Rightarrow T_n = E_0 \left[\frac{\lambda}{(\lambda^2 - L_n^2)^{1/2}} - 1 \right]$$

(= total energy - rest mass energy).

➤ The final energy is thus predetermined by the geometry of the machine – apart from inevitable energy spread arising from the phase stability of the machine.



Alvarez DTL Illustrating the decreasing DT diameter increasing with DT length to maintain cavity resonance

The energy gain is obtained in terms of the transit factor. The electric field is of the form:

$$\begin{aligned}\varepsilon &= \varepsilon_m(z) \sin\left(\frac{\omega_{rf} z}{v} + \phi\right) \\ &= \varepsilon_m(z) \sin\left(\frac{2\pi z}{L} + \phi\right)\end{aligned}$$

where $\omega_{rf} = 2\pi c/\lambda$ and the cell length $L = \beta\lambda$. The origin is chosen according to:

$$\int_L \varepsilon_m(z) \sin\left(\frac{2\pi z}{L}\right) dz = 0$$

Thus, the origin lies at the geometrical center of the gap only if the field is symmetrical.

The energy gain is given by:

$$\begin{aligned}\Delta E &= q \int_L \varepsilon_m \sin\left(\frac{2\pi z}{L} + \phi\right) dz \\ &= q \cos \phi \int_L \varepsilon_m \sin\left(\frac{2\pi z}{L}\right) dz + q \sin \phi \int_L \varepsilon_m \cos\left(\frac{2\pi z}{L}\right) dz.\end{aligned}$$

The first term vanishes as a consequence of the definition of the electrical center:

$$\Delta E = q \sin \phi \left[\frac{\int_L \varepsilon_m(z) \cos\left(\frac{2\pi z}{L}\right) dz}{\int_L \varepsilon_m(z) dz} \right] \int_L \varepsilon_m dz - \text{here quantity in parenthesis is the transit factor.}$$

Thus, we obtain:

$$\Delta E = qF \sin \phi \left[\frac{\int_L \epsilon_m(z) dz}{\int_L dz} \right] \int_L dz.$$

The transit factor, $F = \left[\frac{\int_L \epsilon_m(z) \cos(2\pi z/L) dz}{\int_L \epsilon_m(z) dz} \right]$ is evaluated with a suitable

computer code, such as 'superfish'. The remaining term in parenthesis is the mean value of the field, averaged over a cell and this finally gives an expression for the energy gain:

$$\Delta E = qF \epsilon_{m,av} L \sin \phi.$$

- A correctly adjusted Alvarez linac maintains a constant value of $\epsilon_{m,av}$ from end to end of the entire structure.
- In general, the transit factor, F , is almost constant.
- Thus, the energy gained, for the synchronous particle, increases from gap to gap (as L increases correspondingly) –in contrast to the Wideroe accelerator in which the energy gain per gap is constant.

➤ However, the increments of momentum are constant and we show this below.

The total energy is given by:

$E^2 = E_0^2 + p^2 c^2$ and on differentiating we obtain the energy increment:

$\Delta E = c^2 p \Delta p / E$. Also,:

$$\frac{E^2 - E_0^2}{E^2} = \frac{p^2 c^2}{E^2} = \beta^2 \Rightarrow \beta = \frac{pc}{E}.$$

Thus, the incremental energy change is given in terms of the momentum change:

$$\Delta E = c\beta\Delta p$$

Equating this to the previous expression, $\Delta E = qF\varepsilon_{m,av} L \sin \phi$, we obtain:

$$\Delta p = qF\varepsilon_{m,av} \frac{\lambda}{c} \sin \phi$$

This is very nearly an exact constant, since F varies only slightly from cell to cell.

Therefore, the momentum is a linear function of the number of cells and, at the n th cell:

$$p_n = \eta qF\varepsilon_{m,av} \frac{\lambda}{c} \sin \phi$$

and $\eta_n = \frac{P_n}{M_0 c} = \eta C$ (where we have introduced $C \equiv qF\epsilon_{m,av}\lambda \sin\phi / E_0$).

Now, we have $1 + \eta_n^2 = \gamma_n^2$, so $\sqrt{1 + \eta_n^2} = \gamma_n = 1 + T_n/E_0$ and solving for the kinetic energy T_n :

$$T_n = E_0 \left[\sqrt{1 + \eta_n^2} - 1 \right]$$

$$T_n = E_0 \left[\sqrt{1 + \eta^2 C^2} - 1 \right]$$

However, recall: $T_n = E_0 \left[\frac{\lambda}{(\lambda^2 - L_n^2)^{1/2}} - 1 \right]$ and thus the final kinetic energy depends on E_0 and the mechanical parameters of the accelerator. Thus, relating this to the above equation, leads us to the conclusion that C is similarly determined once the machine is fabricated.

➤ Hence, the average peak field $\epsilon_{m,av}$ is prescribed once ϕ is chosen.

Cell Length Design

- For ion DTL accelerators the change in particle mass with velocity initially is a small effect (proton rest mass ~ 938 MeV) and thus we make the realistic approximation that the constant increments of momentum, discussed previously, may be replaced by a constant velocity increment ($\Delta p \sim m_0 \Delta v$).
- For particles starting from rest this makes: $L_1 = \tau v_1 = \tau \Delta v$, $L_2 = \tau v_2 = \tau (v_1 + \Delta v)$ and in general $L_n = n \tau \Delta v$ (where $\tau = \lambda/c$).
- We end up with the lengths of the cells increasing in proportion to the first power of the series of integers.
- This leads to unrealistically small initial cells. Thus, a DTL linac is preceded by an accelerator such as an RFQ (or prior to the invention of RFQs a Cockcroft Walton) with an energy of 500 to 800 keV.

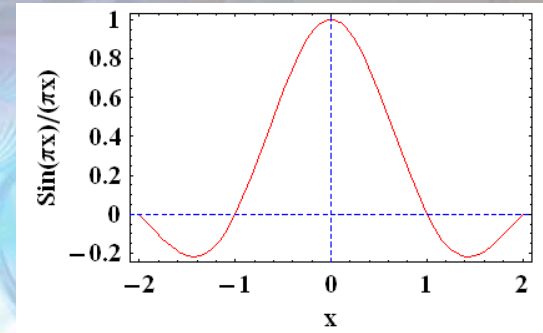
Transit Factor

➤ Inside the tubes the e.m. field is cut-off and hence we can set it to zero in this region and in the gap it is constant to a good approximation.

Thus the transit factor can be explicitly evaluated:

$$F = \frac{\epsilon_m \int_{-g_n/2}^{g_n/2} \cos(2\pi z / L_n) dz}{\epsilon_m \int_{-g_n/2}^{g_n/2} dz} = \text{sinc}(g_n / L_n)$$

where $\text{sinc}(x) = \frac{\sin(\pi x)}{\pi x}$



➤ The sinc function is of course peaked near $x \sim 0$ and hence the energy gain reduces with increasing values of g_n / L_n .

➤ It is thus to have the gap length as short as possible provided electrical breakdown is avoided.

➤ In practice the ratio of gap to cell length lies in the range 1/4 to 1/3.

➤ Also, the average potential difference across a cell is given by $\epsilon_{m,av} L_n$. The field is zero with the gap and has a finite average $\epsilon_{m,g,av}$ within the gap. The same potential difference appears across the gap: $\epsilon_{m,g,av} g_n = \epsilon_{m,av} L_n$.

➤ The field in the gap is increased above the average value in the ratio: L_n / g_n

Cavity Tuning

- The drift tubes decrease the volume available to the electric field at a region where it is strongest and at a region where the magnetic field is the weakest.
- Thus, the drift tubes detune the frequencies of the cells.
- From repeated measurements an empirical relationship indicating this interdependence has been obtained:

$$\frac{g_n}{L_n} = -C_1 + C_2 \frac{D}{\lambda} + C_3 \frac{L_n}{\lambda} + C_4 \frac{d_n}{\lambda}$$

- Here the Cs are constants, determined for a specific DTL geometry, D is the cavity diameter and d_n , that of the cylindrical drift tube.

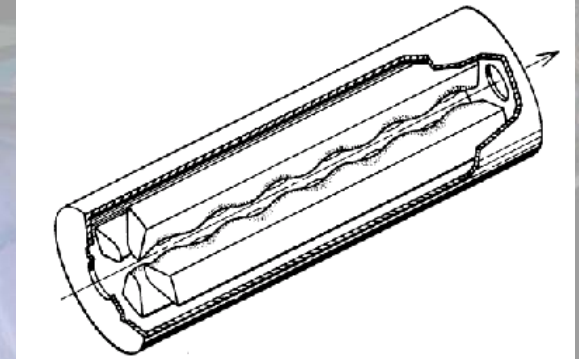
- Thus, for a fixed RF frequency and for fixed D and d_n it is necessary for the ratio g_n/L_n to increase as the cell length increases along the DTL linac. This procedure can only be carried out to a limited extent as there is an energy loss associated with decreasing the transit factor as increased g_n/L_n .

- Alternatively, for a fixed g_n/L_n then as L_n increases the cells are re-tuned by decreasing the diameter of each drift tube. This is limited by how small is practical to allow the beam to transit each cavity without interception.

- Finally, it is to be noted that tuning posts are also often inserted into the cells to achieve a flat field.

Radio Frequency Quadrupole (RFQ)

➤ In 1970 two Russian scientists, I.M. Kapchiski and V.A. Tepliakov, proposed an rf linear accelerator structure with a symmetry corresponding to that of an electric quadrupole. This rf structure, which has become known world-wide as the radio frequency quadrupole (RFQ) linac.



➤ The RFQ's electric fields are produced by the rf fields applied to four electrodes that are collinear with the beam axis. By modulation of this pure quadrupole focussing geometry an axial field component can be introduced in the regions between adjacent "hills and valleys" which then causes a dc beam injected into the structure along its axis to be focused, bunched and accelerated simultaneously by the rf fields.

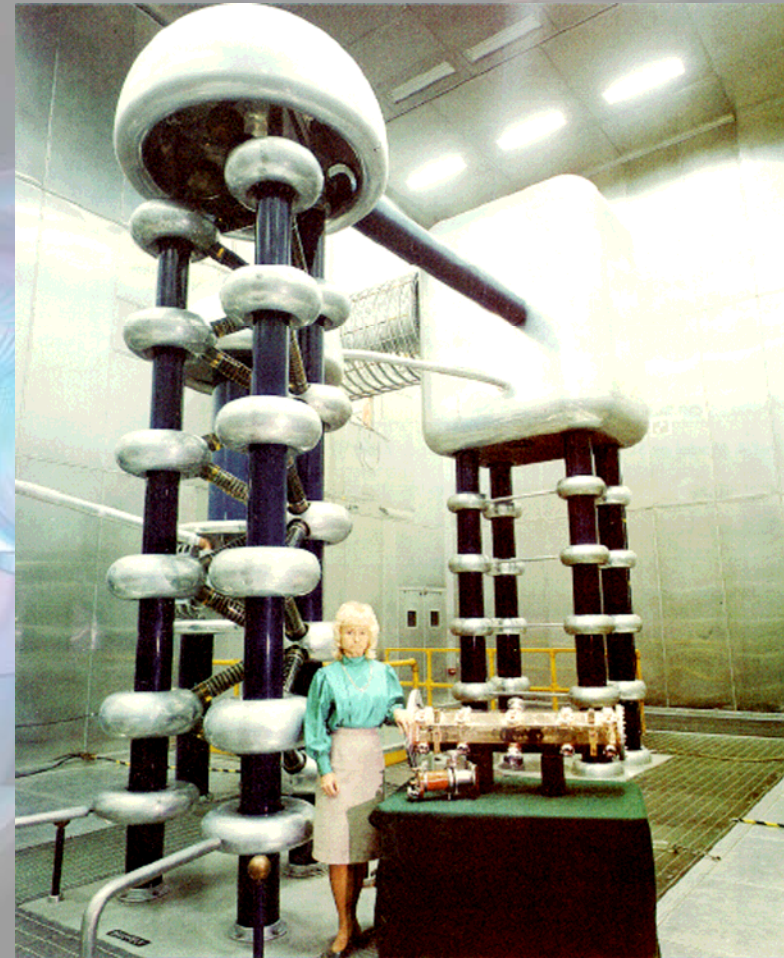
➤ This unique rf accelerator structure has the property of the Wideröe linac that particles are only accelerated in every other gap. However, unlike the Wideröe structure, the beam does not get shielded from the field as it changes, but rather the particles drift through a region where the four vanes have the same geometry and where only a focusing field is present when the electric field changes polarity.

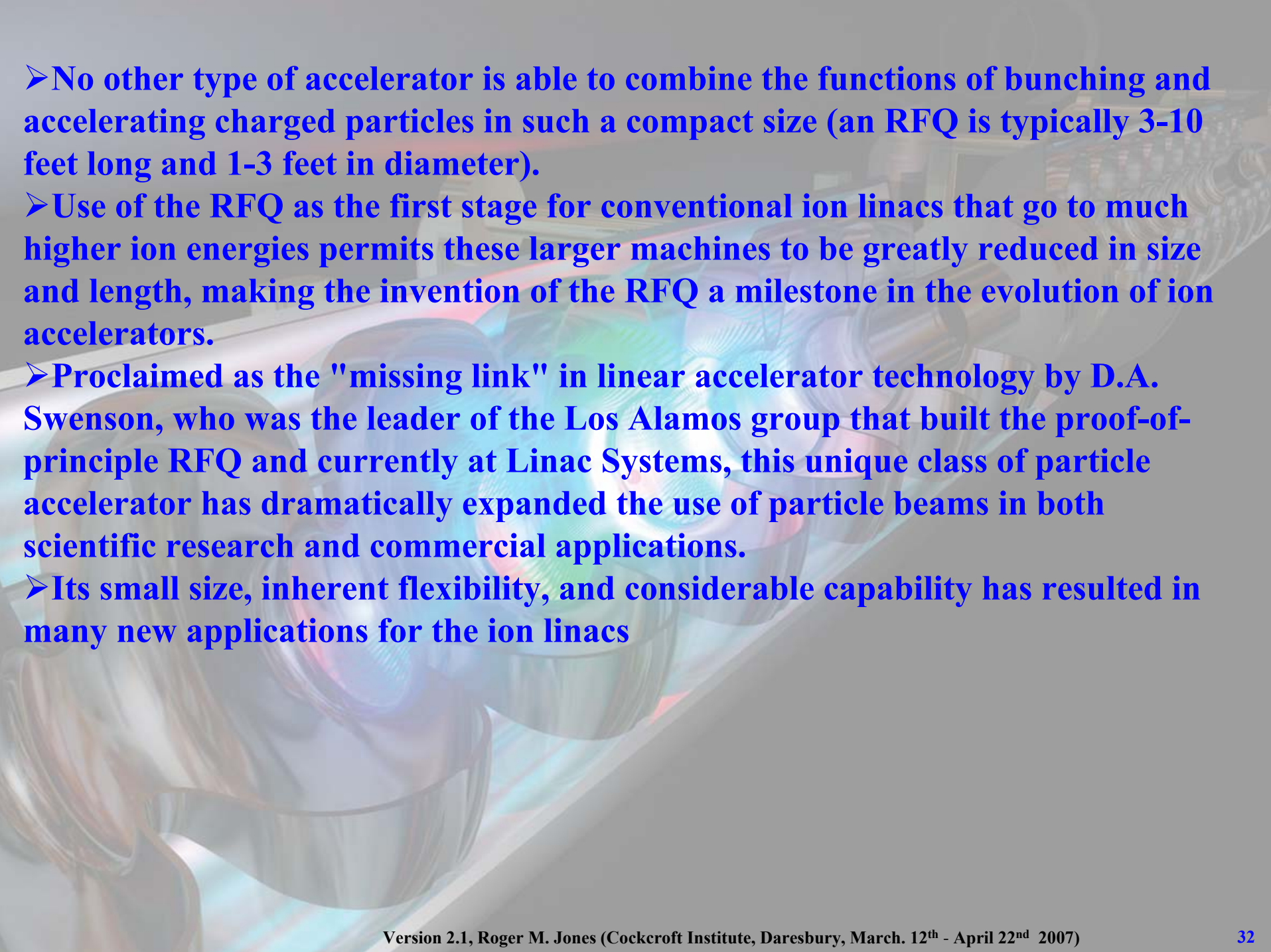
Radio Frequency Quadrupole (RFQ)

➤ In addition, in 1975 after the highly successful completion of the 800 MeV proton linac at Los Alamos (the Los Alamos Meson Physics Facility-LAMPF), scientists at that laboratory began a program sponsored by the National Cancer Institute to vastly reduce the size of such conventional accelerators to make it possible to use proton linacs in a hospital-based facility for pion therapy.

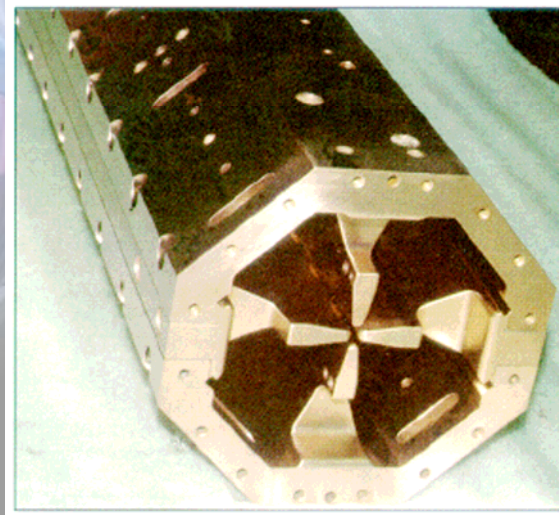
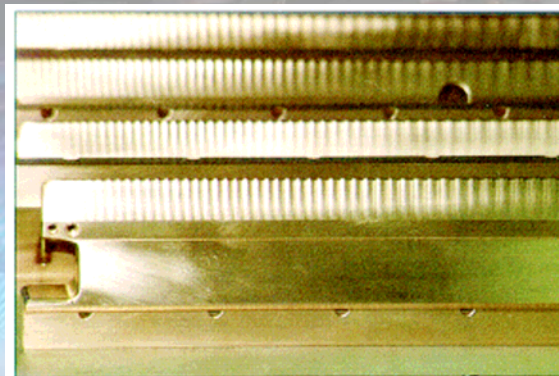
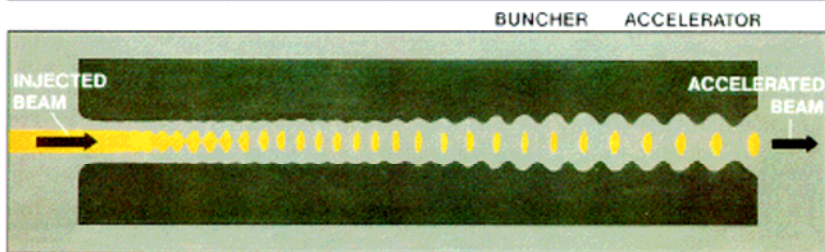
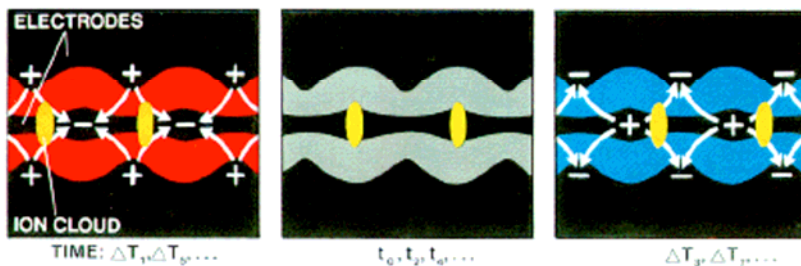
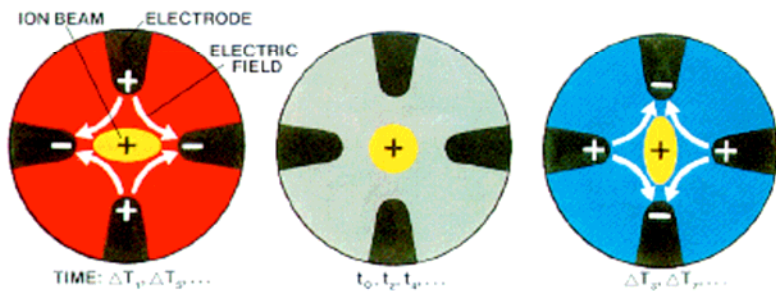
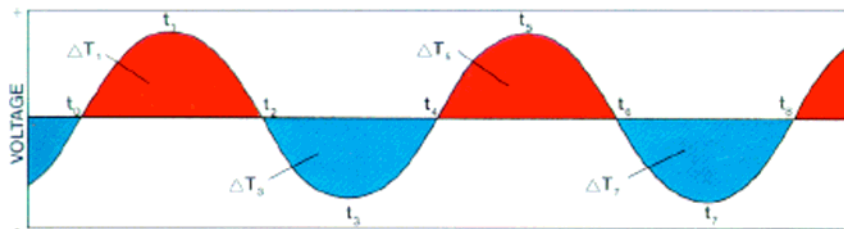
➤ While the PIGMI (Pion Generator for Medical Irradiation) program did not result in the construction of such a system before it was terminated in 1981, it did have a significant impact on modern commercial ion linacs.

➤ Besides the testing of the first RFQ linac, the use of a higher frequency (425 MHz) to make the drift tube linac smaller in size and shorter in length was demonstrated, along with the use of rare-earth permanent magnet quadrupoles that could fit in the much smaller drift tubes found in such a system.

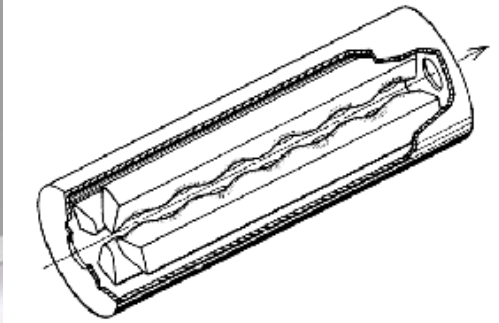


- 
- No other type of accelerator is able to combine the functions of bunching and accelerating charged particles in such a compact size (an RFQ is typically 3-10 feet long and 1-3 feet in diameter).
 - Use of the RFQ as the first stage for conventional ion linacs that go to much higher ion energies permits these larger machines to be greatly reduced in size and length, making the invention of the RFQ a milestone in the evolution of ion accelerators.
 - Proclaimed as the "missing link" in linear accelerator technology by D.A. Swenson, who was the leader of the Los Alamos group that built the proof-of-principle RFQ and currently at Linac Systems, this unique class of particle accelerator has dramatically expanded the use of particle beams in both scientific research and commercial applications.
 - Its small size, inherent flexibility, and considerable capability has resulted in many new applications for the ion linacs

Radio Frequency Quadrupole (RFQ)



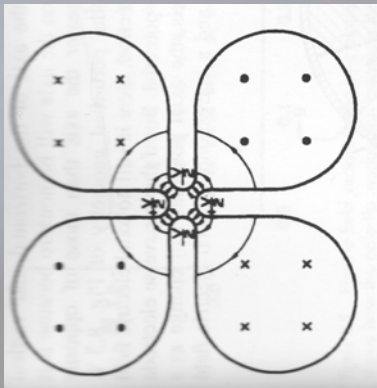
Radio Frequency Quadrupole (RFQ)



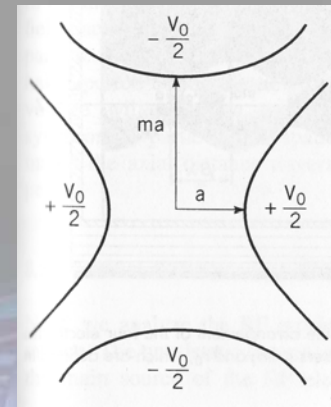
Schematic of RFQ illustrating 4 electrodes with radial perturbations

- The RFQ is a relatively new type of linear accelerator.
- It can be traced to the original paper by K-T (I.M. Kapchinskiy, V.S. Teliakov), Prib. Tekh. Eksp. 2, 19-22 (1970).
- It is now quite routinely used to pre-accelerate ions.
- Electrons, in contrast can be accelerated to sufficiently high energies suitable for direct injection into a linac.
- It consists of four vanes which provide the unique function of both focussing and accelerating in a remarkably compact structure.
- Thus, the need for large unwieldy high voltage electrostatic pre-injector structures is eliminated.
- In an RFQ no drift tubes or magnetic quadrupole lenses are used.
- However, the beam is accelerated by longitudinal fields and focussed by RF electric quadrupole fields that are determined purely from the electrode geometry of the structure.
- These electrodes either consist of vanes or rods.

Focussing

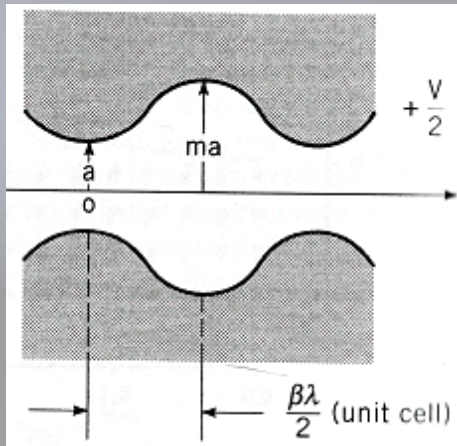


Equally
Spaced
Electrodes



Non-
Equally
Spaced
Electrodes

- Firstly, consider the case of four equally spaced electrodes.
- Apply a voltage $V_0 \cos \omega t/2$ with a polarity that alternates in quadrupole manner.
- Clearly, off-axis particles experience an alternating RF quadrupole field that is focussing.
- There is of course an RF magnetic field also. However, at low-velocities – in which the RFQ was designed to operate in the first place – the electric force is stronger than the magnetic force.
- However, the present configuration provides no acceleration!
- If we consider the modified geometry in which the horizontal electrode spacing differs from the vertical spacing then we find that potential on the axis is now longer zero.
- If we maintain this along the axis of the accelerator then the potential remains constant on axis and there is no electric field.



Unit Cell of RFQ.
Modulation parameters indicated

- If we allow the radius of the vanes to also to vary along the axis of the accelerator, then the potential will also vary.
- This provides an axial accelerating electric field. In practise this is varied in a sinusoidal manner.
- The horizontal and vertical electrodes are 180 out of phase.
- At a particular instant in time the voltage down the axis of the accelerator has a sinusoidal profile.

- As in any RF linear accelerator, the reason for the time dependent field is clear –without time dependence the overall energy gain would be zero as the particles would receive equal amounts of acceleration as well as deceleration.
- The spatial period of the electrode displacements must match the axial distance tranversed by a synchronous particle during one RF period.

Potential Distribution

- We analyse the RFQ using a quasi-static approximation.
- This is valid provided the main source of the RF field is the electric charge on the four vanes and the contribution from the time-varying magnetic field –given by Faraday’s law- is sufficiently small that it can be ignored.
- This is indeed valid provided the electrode displacements from the axis are small compared to the RF wavelength.
- We will treat the vane displacements as periodic, even though in practise they are not quite periodic as the electron gains energy the cell length needs to increase to maintain synchronism.
- This approximation corresponds to assuming the rate of acceleration is small compared to the distance the particle moves in one RF period of the wave.
- The model assumes a minimum vane spacing of “a” and a maximum of “ma”.
- The unit cell is of length $\beta\lambda/2$ –there being two of these per modulation period
- Every other cell may contain a bunch for acceleration.

In cylindrical-polar coordinates the time dependent scalar potential is :

$$U(r, \theta, z, t) = V(r, \theta, z) \sin(\omega t + \phi)$$

where $\omega/2\pi$ is the RF frequency, ϕ the initial phase of the potential and $V(r, \theta, z)$ is a solution of Laplace's equation, in cylindrical coordinates given by:

$$\frac{\partial^2 V}{\partial r^2} + \frac{1}{r} \frac{\partial V}{\partial r} + \frac{1}{r^2} \frac{\partial^2 V}{\partial \theta^2} + \frac{\partial^2 V}{\partial z^2} = 0$$

where in Cartesian coordinates $x=r\cos\theta$ and $y=r\sin\theta$.

When considering electrode displacement that vary along the z-axis we are interested in 3-D solutions that depend on z.

When we are concerned with the focussing we are interested in symmetric solutions.

Using the method of separation of variables for each case we have:

$$V(r, \theta, z) = \sum_{s=0}^{\infty} A_s r^{2(2s+1)} \cos[2(2s+1)\theta] + \sum_{n=1}^{\infty} \sum_{s=0}^{\infty} A_{ns} I_{2s}(knr) \cos 2s\theta \sin knz$$

To obtain an the surface of an arbitart geometry requires many terms in the infinite series. However, in practise (and as was proposed in the original K-T paper) we carefully chose the geometry such that only a few terms are necessary. This allows analytical expression for the field and beam stability to be obtained.

Thus, only taking two terms in the summations, namely $s=0$ the quadrupole term and $n=1,s=0$, the monopole term from the second summation:

$$V(r,\theta,z)=A_0r^2 \cos 2\theta + A_{10}I_0(kr) \cos kr$$

where A_0 and A_{10} are constants determined from the electrode geometry, $k=2\pi/L$, L the period of the modulation ($L=\beta_s\lambda$, with β_s the velocity of the synchronous particle).

We will be interested in small displacement and we will have occasion to use:

$$I_0(\alpha) \sim 1 + \alpha^2/4, \quad I(\alpha) \sim \alpha/2.$$

In order to determine the two constant A_0 and A_{10} we equate the potential at the tips of the electrodes. Recall that they are π out of phase, so that at $z=0$ and $\theta=0$ we have

$$V(a,0,0) = V_0/2 \text{ and conversely at } \theta=\pi/2, V(ma,\pi/2,0) = -V_0/2.$$

Using these boundary conditions in the above expansion at $\theta=0$:

$$\frac{V_0}{2} = A_0 a^2 + A_{10} I_0(ka)$$

and at $\theta=\pi/2$:

$$-\frac{V_0}{2} = -A_0 (ma)^2 + A_{10} I_0(kma)$$

And these 2 simultaneous equations are readily solved for the constants

A_0 and A_{10} :

$$A_0 = \frac{V_0}{2a^2} \frac{I_0(ka) + I_0(kma)}{m^2 I_0(ka) + I_0(kma)}$$

$$A_{10} = \frac{V_0}{2} \frac{m^2 - 1}{m^2 I_0(ka) + I_0(kma)}$$

We now introduce dimensionless constants:

$$X = \frac{I_0(ka) + I_0(kma)}{m^2 I_0(ka) + I_0(kma)}$$

$$A = \frac{m^2 - 1}{m^2 I_0(ka) + I_0(kma)}$$

And this makes $A_0 = XV_0 / 2a^2$ and $A_{10} = AV_0 / 2$. Thus, time dependent potential becomes:

$$U(r,\theta,z) = \frac{V_0}{2} \left[X \left(\frac{r}{a} \right)^2 \cos 2\theta + AI_0(kr) \cos kz \right] \sin(\omega t + \phi)$$

where the time-dependent voltages on the horizontal and vertical electrodes are: $V_0 \sin(\omega t + \phi) / 2$ and $-V_0 \sin(\omega t + \phi) / 2$, respectively.

Also, using $x=r\cos\theta$ and $y=r\sin\theta$ it is straightforward to also express this in Cartesian coordinates

$$U(x,y,z) = \frac{V_0}{2} \left[X \left(\frac{x^2 - y^2}{a^2} \right) + AI_0(kr) \cos kz \right] \sin(\omega t + \phi)$$

The geometry of the electrodes can now be obtained from the equipotential surfaces.

In this approximation, the transverse cross-sections are hyperbolas. At $z = \beta_s \lambda / 4$, half way through the unit cell, the RFQ has exact quadrupole symmetry, the tips of the vanes have equal radius $r_0 = aX^{-1/2}$.

In general the tip at $y=0$ is described by:

$$1 = \frac{X}{a^2} x^2 \cos 2\theta + A I_0(kx) \cos kz$$

and the tip at $x=0$:

$$-1 = -\frac{X}{a^2} y^2 \cos 2\theta + A I_0(ky) \cos kz$$

Clearly, other other shapes are also possible to provide a sinusoidal modulation in the potential.

In practise, care must be taken to ensure that the closest approach of the vanes does not give rise to breakdown.

Electric Field

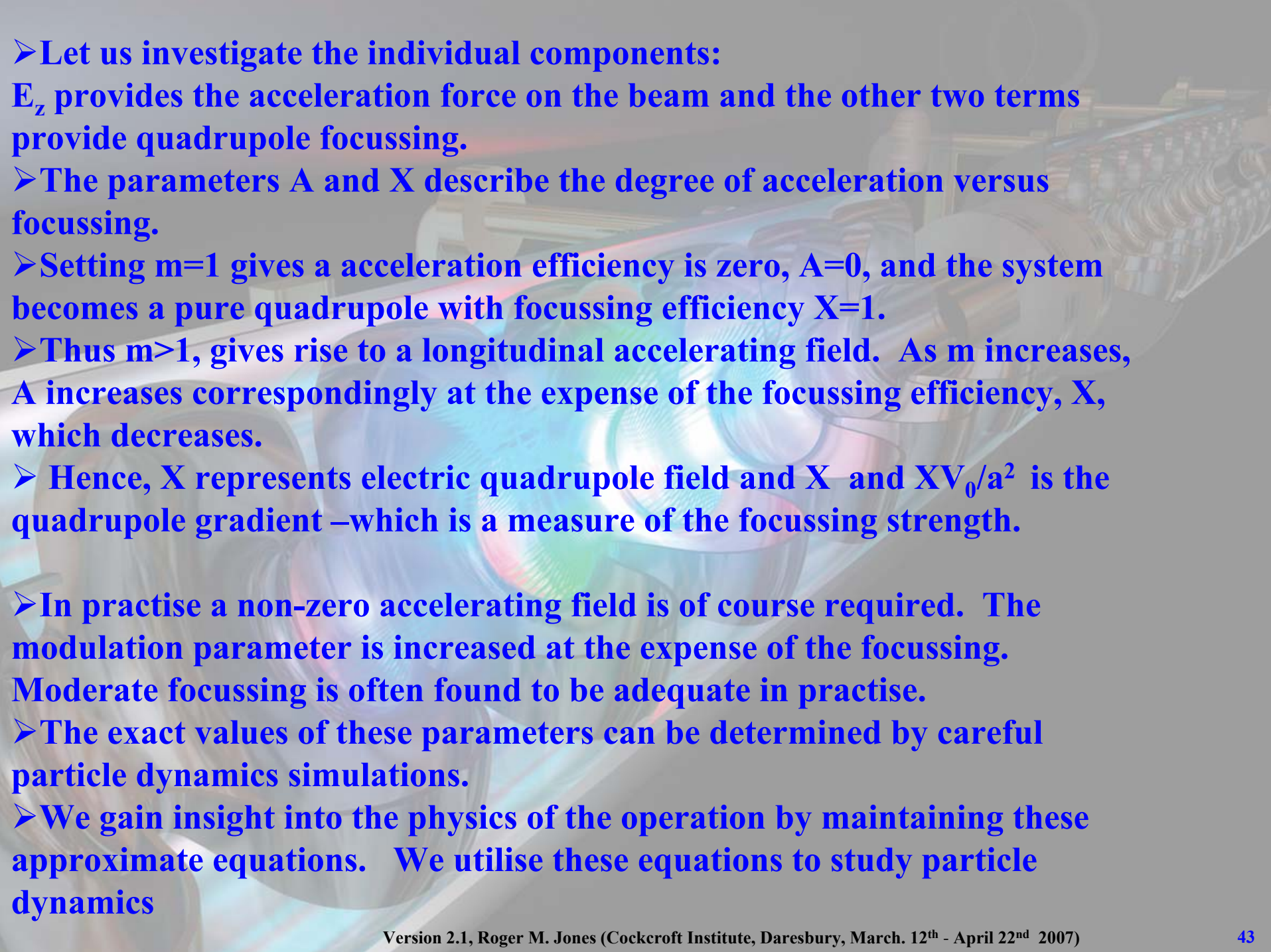
The electric field is given by the gradient of the potential:

$E = -\nabla U$ and thus from the derivative of the Cartesian representation:

$$E_x = -\frac{XV_0}{a^2} x - \frac{kAV_0}{2} I_1(kr) \frac{x}{r} \cos kz$$

$$E_y = \frac{XV_0}{a^2} y - \frac{kAV_0}{2} I_1(kr) \cos kz$$

$$E_z = \frac{kV_0A}{2} I_0(kr) \sin kz$$

- 
- Let us investigate the individual components:
 E_z provides the acceleration force on the beam and the other two terms provide quadrupole focussing.
 - The parameters A and X describe the degree of acceleration versus focussing.
 - Setting $m=1$ gives a acceleration efficiency is zero, $A=0$, and the system becomes a pure quadrupole with focussing efficiency $X=1$.
 - Thus $m>1$, gives rise to a longitudinal accelerating field. As m increases, A increases correspondingly at the expense of the focussing efficiency, X , which decreases.
 - Hence, X represents electric quadrupole field and X and XV_0/a^2 is the quadrupole gradient –which is a measure of the focussing strength.
 - In practise a non-zero accelerating field is of course required. The modulation parameter is increased at the expense of the focussing. Moderate focussing is often found to be adequate in practise.
 - The exact values of these parameters can be determined by careful particle dynamics simulations.
 - We gain insight into the physics of the operation by maintaining these approximate equations. We utilise these equations to study particle dynamics

Synchronous Acceleration

- For small transverse offsets it is sufficient to neglect this effect in calculating the energy gain.
- Within a unit cell we assume the radial position and velocity are constant
- To calculate the energy gain ΔW with arbitrary normalised velocity β' we replace $\omega t = 2\pi z / (\beta' \lambda)$ and integrate the E-field experienced by the particle $E_z \sin(\omega t + \phi)$ over the cell length:

$$\Delta W = \frac{qAV_0 I_0(kr)}{2} \int_0^l \sin kz \sin(k'z + \phi) dz$$

where $k' = 2\pi/\beta'\lambda$, $k = 2\pi/\beta_s\lambda$ and $l = \beta_s\lambda/2$.

Maximum acceleration occurs when a particle travels from the centre of one cavity to the next such that the field reverse polarity -in other words in one half RF period.

This is the synchronous particle.

Clearly synchronism corresponds to $\beta' = \beta_s$ and the energy gain is given by:

$$\Delta W = \frac{q\pi AV_0 I_0(kr)}{4} \cos \phi$$

Δ The phase ϕ when the particle is at the centre of the cell is referred to as the particle phase; at $\phi=0$ the electric field is at a peak.

We can also write energy gain in terms of the transit factor. Firstly, calculate spatial average of the peak axial accelerating field over an RFQ unit cell ($l=\beta\lambda/2$):

$$E_0 = \frac{1}{l} \int_0^l E_z dz = \frac{1}{l} \int_0^l \frac{kV_0 A}{2} \sin kz dz = \frac{2AV_0}{\beta\lambda}$$

This expresses average field as a ratio of the effective voltage AV_0 over a unit cell of length l . The transit factor is given by:

$$T = \frac{\int_0^l E_z \sin kz dz}{\int_0^l E_z dz} = \frac{\int_0^l \sin^2 kz dz}{\int_0^l \sin kz dz} = \frac{\pi}{4}$$

Combining these results we finally obtain the energy gain:

$$\Delta W = qE_0 T I_0(kr) l \cos \phi$$

Longitudinal Beam Dynamics

Since $\Delta W = qE_0 T I_0(kr) l \cos \phi$ it is straightforward to show that:

$$\frac{d}{dz}(W - W_s) = qE_0 T I_0(kr) [\cos \phi - \cos \phi_s]$$

The equation for the synchronous phase requires a little more thought and algebraic manipulation

Consider the phase ϕ_n at cell n. This is related to that at the previous cell by:

$$\phi_n = \phi_{n-1} + \frac{\omega L_{n-1}}{\beta_{n-1} c}, \text{ where } L_{n-1} = \beta_{s,n-1} \lambda. \text{ We now evaluate the incremental phase change:}$$

$$\Delta(\phi - \phi_s)_n = \Delta\phi - \Delta\phi_s$$

$$= \lambda \frac{\omega}{c} \beta_{s,n-1} \left(\frac{1}{\beta_{n-1}} - \frac{1}{\beta_{s,n-1}} \right) = 2\pi \beta_{s,n-1} \left(\frac{1}{\beta_{n-1}} - \frac{1}{\beta_{s,n-1}} \right)$$

Making a Taylor expansion in $\delta\beta$:

$$\frac{1}{\beta} - \frac{1}{\beta_s} = \frac{1}{\beta_s + \delta\beta} - \frac{1}{\beta_s} \approx -\frac{\delta\beta}{\beta_s^2}$$

and from the usual relation $W=\gamma mc^2$ we obtain :

$$\delta\beta = \frac{\delta W}{mc^2 \gamma_s^3 \beta_s}$$

$$\Rightarrow \Delta(\phi - \phi_s)_n = -2\pi \frac{W_{n-1} - W_{s,n-1}}{mc^2 \gamma_{s,n-1}^3 \beta_{s,n-1}^2}$$

Now we make a transition from integral discrete differences to derivatives:

$$\Delta(\phi - \phi_s) \rightarrow \frac{d}{dn}(\phi - \phi_s) \text{ and } \Delta(W - W_s) \rightarrow \frac{d}{dn}(W - W_s)$$

$$\text{with } n = \frac{z}{\beta_s \lambda} \text{ we have } \frac{d}{dn}(\phi - \phi_s) \rightarrow \beta_s \lambda \frac{d}{dz}(\phi - \phi_s) \text{ and}$$

$$\frac{d}{dn}(W - W_s) \rightarrow \beta_s \lambda \frac{d}{dz}(W - W_s).$$

Thus, we obtain:

$$\frac{d}{dz}(\phi - \phi_s) = -\frac{2\pi}{mc^2 \gamma_s^3 \beta_s^3 \lambda} (W - W_s)$$

For low-energy particles $\gamma \sim 1$:

$$\frac{d}{dz}(\phi - \phi_s) = -\frac{2\pi}{mc^2\beta_s^3\lambda}(W - W_s)$$

Taking the derivative of this wrt to z and using the energy relation

$$\left(\frac{d}{dz}(W - W_s) = qE_0 T I_0(kr) [\cos \phi - \cos \phi_s] \right) \text{ gives:}$$

$$\frac{d^2}{ds^2}(\phi - \phi_s) = q2\pi \frac{2AV_0}{\beta_s\lambda} \frac{\pi I_0(kr)}{4 mc^2\beta_s^3} 2 \sin\left(\frac{\phi - \phi_s}{2}\right) \sin\left(\frac{\phi + \phi_s}{2}\right)$$

$$\Rightarrow \frac{d^2}{ds^2}\left(\frac{\phi - \phi_s}{2}\right) + \frac{\pi^2 qAV_0 I_0(kr) \sin(-\phi_s)}{mc^2\beta_s^4\lambda^2} \sin\left(\frac{\phi - \phi_s}{2}\right) = 0$$

where we have used $\phi \sim \phi_s$. Thus, we associate this phase with SHM and this has a longitudinal wavenumber:

$$k_1^2 = \frac{\pi^2 qAV_0 I_0(kr) \sin(-\phi_s)}{mc^2\beta_s^4\lambda^2}.$$

Hence, stable SHM occurs provided $-\pi < \phi_s < 0$.

Transverse Beam Dynamics

- The strength of the RFQ lies in its superior focussing for low energy ions.
- The focussing or confinement of off-axis particles is an example of alternating gradient focussing. In conventional linacs, the polarity of the focussing varies spatially. However, in an RFQ the polarity of the focussing varies in time rather than space.
- To analyse the behaviour we consider small displacement of off-axis low-energy ions. Thus, the non-relativistic equation of motion is given by:

$$\ddot{x} + \left(\frac{qXV_0}{ma^2} + \frac{qk^2AV_0}{4m} \cos kz \right) x \sin(\omega t + \phi) = 0$$

where $\ddot{x} = d^2x/dt^2$

- The first term in parenthesis is the quadrupole term.
- And the second term is the transverse field associated with electrode modulation that produces the required longitudinal fields.

This latter term is proportional to:

$$\cos\omega t \sin(\omega t + \phi) = \frac{\sin(\phi) + \sin(2\omega t + \phi)}{2}$$

For unit cell consisting of a peak to a trough in vane undulations this term goes through one complete RF period and hence it averages out to zero.

Thus, we ignore this term and the new equation of motion becomes:

$$\ddot{x} + \left(\frac{qXV_0}{ma^2} \sin(\omega t + \phi) + \frac{qk^2 AV_0}{8m} \sin\phi \right) x = 0$$

This is in the form of the Mathieu equation. A smooth approximation is obtained in the form of a trial solution

$$x = (C_1 \sin\Omega t + C_2 \cos\Omega t) + \varepsilon \sin(\omega t + \phi)$$

where C_1 and C_2 are constants and Ω and ε are two further parameters, such that

$\Omega \ll \omega$ and $\varepsilon \ll 1$. The first term in parentheses represents the averaged or smoothed particle trajectory, in which the particles oscillate at the "betatron frequency" Ω .

The remaining factor in brackets is the "flutter function or flutter amplitude" ε .

To obtain these two parameters we will substitute the trial solution into the equation of motion. For simplicity we $C_1 = 1$ and $C_2 = 0$, differentiate the trial solution twice, neglect second order terms ($\varepsilon\Omega/\omega$ and Ω^2/ω^2):

$$\ddot{x} \cong -\varepsilon\omega^2 \sin\Omega t \sin(\omega t + \phi)$$

An approximate solution of the equation of motion is obtained by choosing

the flutter function:
$$\varepsilon \cong \frac{qXV_0}{m\omega^2 a^2} = \frac{1}{4\pi^2} \frac{qXV_0 \lambda^2}{mc^2 a^2}$$

Similarly, to study the betatron oscillations we substitute the trial solution into the equation of motion, and average over an RF period:

$$\bar{\ddot{x}} \cong -\Omega^2 \sin\Omega t$$

Thus, the smooth approximation implies the average particle satisfies the SHM equation:

$$\bar{\ddot{x}} + \Omega^2 \bar{x} = 0$$

with
$$\Omega^2 \cong \frac{1}{2} \left(\frac{qXV_0}{m\omega a^2} \right)^2 + \frac{qk^2 V_0 A \sin\phi}{8m}$$

The first term is always positive and it represents the quadrupole focussing, and the second term represents the RF defocus term -depending on the acceleration efficiency parameter A .

If the quadrupole term is larger compared to the RF defocussing term then the transverse motion becomes decoupled from the longitudinal motion and Ω is approximately the same for all phases.

It is convenient to refer to the phase advance per focussing period:

$$\sigma_0 = \Omega\lambda / c :$$

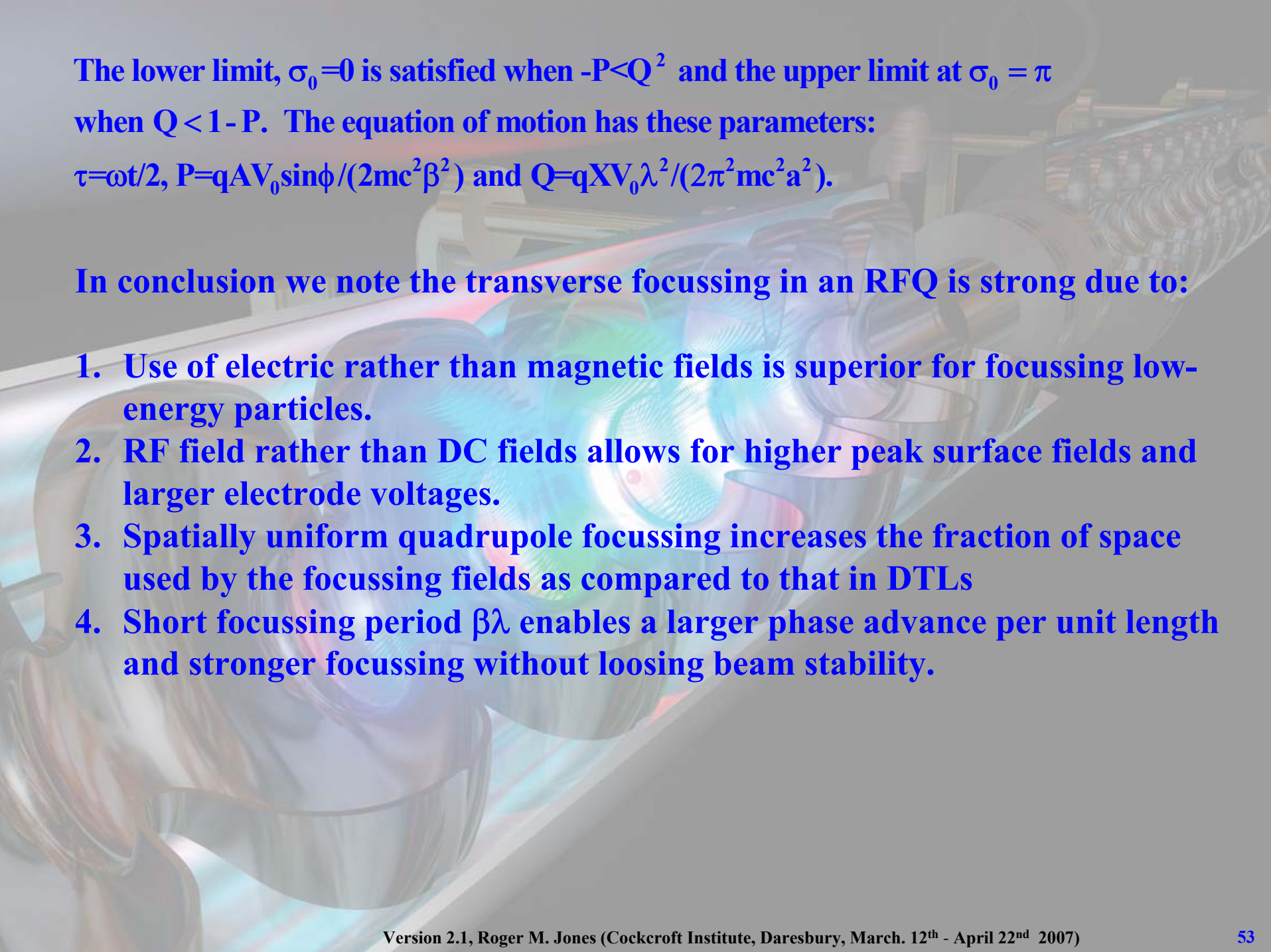
$$\sigma_0^2 \cong \frac{1}{8\pi^2} \left(\frac{qXV_0\lambda^2}{mc^2a^2} \right)^2 + \frac{\pi^2qV_0A\sin\phi}{2mc^2\beta^2}$$

Stability criteria depend on σ_0 . The beam is in fact stable when $\sigma_0^2 > 0$. In the phase range: $-\pi/2 \leq \phi \leq 0$ (i.e. the condition for simultaneous acceleration and longitudinal focussing), the second term is negative, and this reduces the net focussing.

For $\phi=0$, corresponding to the peak of the accelerating waveform the defocussing effect vanishes but it is a maximum at $\phi=-\pi/2$. If the second term exceeds the first then stable beam motion is not possible.

A more accurate treatment of the solution to the Mathieu equation reveals a modified stability criterion: $0 < \sigma_0 < \pi$. The Mathieu equation is written:

$$\frac{d^2x}{d\tau^2} + (P + 2Q\sin 2\tau)x = 0$$



The lower limit, $\sigma_0 = 0$ is satisfied when $-P < Q^2$ and the upper limit at $\sigma_0 = \pi$ when $Q < 1 - P$. The equation of motion has these parameters:
 $\tau = \omega t / 2$, $P = qAV_0 \sin \phi / (2mc^2 \beta^2)$ and $Q = qXV_0 \lambda^2 / (2\pi^2 mc^2 a^2)$.

In conclusion we note the transverse focussing in an RFQ is strong due to:

1. Use of electric rather than magnetic fields is superior for focussing low-energy particles.
2. RF field rather than DC fields allows for higher peak surface fields and larger electrode voltages.
3. Spatially uniform quadrupole focussing increases the fraction of space used by the focussing fields as compared to that in DTLs
4. Short focussing period $\beta \lambda$ enables a larger phase advance per unit length and stronger focussing without losing beam stability.

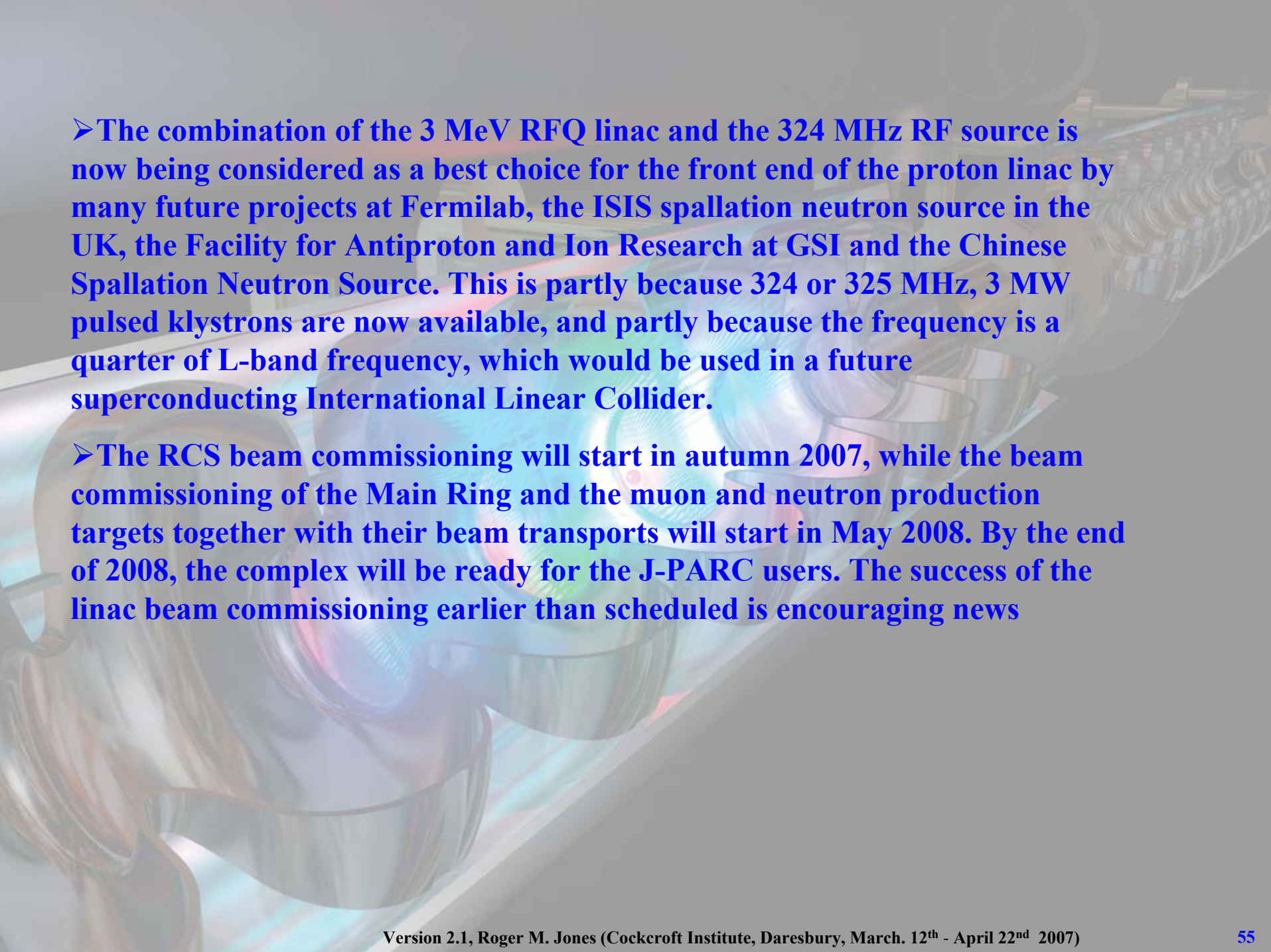
J-PARC linac accelerates hydrogen ions up to 181 MeV design value (CERN COURIER)

➤ On 24 January 2007 the linac for the Japan Proton Accelerator Research Complex (J-PARC) successfully accelerated a beam of negative hydrogen ions up to 181 MeV, the design energy for Phase I of the project. The acceleration to the full energy is three months earlier than scheduled.

J-PARC team

➤ J-PARC, which is a joint project between the High Energy Accelerator Research Organization (KEK) and the Japan Atomic Energy Agency (JAEA), is being built at Tokai, approximately 120 km north of Tokyo. The accelerator system will comprise a 400 MeV proton linac (181 MeV at the first stage of Phase I), a 3 GeV, 25 Hz Rapid-Cycling Synchrotron (RCS), and a 50 GeV Main Ring Synchrotron.





➤ The combination of the 3 MeV RFQ linac and the 324 MHz RF source is now being considered as a best choice for the front end of the proton linac by many future projects at Fermilab, the ISIS spallation neutron source in the UK, the Facility for Antiproton and Ion Research at GSI and the Chinese Spallation Neutron Source. This is partly because 324 or 325 MHz, 3 MW pulsed klystrons are now available, and partly because the frequency is a quarter of L-band frequency, which would be used in a future superconducting International Linear Collider.

➤ The RCS beam commissioning will start in autumn 2007, while the beam commissioning of the Main Ring and the muon and neutron production targets together with their beam transports will start in May 2008. By the end of 2008, the complex will be ready for the J-PARC users. The success of the linac beam commissioning earlier than scheduled is encouraging news